2018

Optimization of Heat Sinks in a Range of Configurations.

Archibald Allswell Amoako
South Dakota State University

OPTIMIZATION OF HEAT SINKS IN A RANGE OF CONFIGURATIONS.

BY:

ARCHIBALD ALLSWELL AMOAKO

A thesis submitted in partial fulfillment of the requirements for the

Master of Science

Major in Mechanical Engineering

South Dakota State University

2018

OPTIMIZATION OF HEAT SINKS IN A RANGE OF CONFIGURATIONS.

ARCHIBALD ALLSWELL AMOAKO

This thesis is approved as creditable and independent investigation by a candidate for the Master of Science in Mechanical Engineering degree and is acceptable for meeting the thesis requirements for the degree. Acceptance of this does not imply that the conclusion reached by the candidate are necessarily the conclusions of the major department.

Jeffrey Doom, Ph.D. Date
Thesis Advisor

Kurt Bassett, Ph.D. Date
Head, Department of Mechanical Engineering

Dean, Graduate School Date

ACKNOWLEDGEMENTS

First, I would like to express my utmost gratitude to my advisor Dr. Jeffery Doom for his support and encouragement during my period of working on my Master's degree and research. Also, huge thanks to Dr. Ross Wilcoxon of Rockwell Collins Inc. who served as my industry advisor at for his input, direction, and knowledge while working on this project. You two have shared so much knowledge with me in the last two years of me working on this project and I pray the good Lord blesses you for your patience and motivation.

In addition to my advisors, I would like to thank my thesis committee consisting of Dr. Zhong Hu and Dr. Adam Hoppe of the chemistry and biochemistry department for their input and comments.

Besides all these wonderful men who have helped me on my journey, I want to thank my parents Archibald Allswell Snr and Sophia Amoako for making it possible to even be able to attain this degree. Thanks for all the prayers and support both financially and emotionally. Also for always being there for me when I need it the most. I would also want to express my gratitude and love to my siblings George, Gladys, Malinda, and Anita for encouraging me and being great role models to look up to. May God bless you all and continue to shower his mercies and favor upon you.

Also, great thanks are in order to the family I call my "American Family" Don, Teresa, and Tyler Rowland. Your love, support, and encouragement are what has kept me strong in hard times when the going was tough. Having a family close by made my journey a lot easier than it would have been. May the good

Lord continue to bless you guys. Also, huge thanks to Princess Ako Adwoa Darko for her support and motivation throughout this process.

Lastly and most importantly I wouldn't be here if not for the mercies, favor, and blessings of my Lord and personal savior. I would like to thank God for seeing me through my journey here at South Dakota State University so far and for the incredible and exciting adventures he has in store for me.

TABLE OF CONTENTS

LIST OF TABLES

LIST OF FIGURES

ABSTRACT

OPTIMIZING HEAT TRANSFER OF HEAT SINKS IN A RANGE OF CONFIGURATIONS.

ARCHIBALD AMOAKO

2018

In this study, different heatsink geometries used for electronic cooling are studied and compared to each other to determine the most efficient. The goal is to optimize heat transfer of the heat sinks studied in a range of configuration based on fin geometry.

Heat sinks are thermal conductive material devices designed to absorb and disperse heat from high-temperature objects (e.g. Computer CPU). Common materials used in the manufacturing of heat sinks are aluminum and copper due to their relatively high thermal conductivity and lightweight [1]. Aluminum is used as the material for the heatsinks studied in this research project.

To start, experimental results from a wind tunnel test conducted were compared to numerical results generated to establish a validation case. Best practices in running numerical simulations on heat sinks along with suitable models for simulating real-world conditions were determined and analyzed. The two main thermal performance-evaluating parameters used in this project are pressure drop (ΔP) and thermal resistance (R).

Thirteen numerical CFD simulations were run on different heatsink fin extrusion geometries including the traditional rectangular plate, arc plate, radial plate, cross pin, draft pin, hexagonal pin, mixed shape pin fin, pin and plate,

separated plate, airfoil plate, airfoil pin, rectangular pin, and square zig-zag plate heat sinks. It was observed that different fin geometries and dimensions affect the performance of heat sinks to varying extents.

The square zig-zag plate heat sink from results obtained had the lowest thermal resistance of 0.25 K/W with the separated plate having the lowest pressure drop of 11.94 Pa. This information is relevant in the selection of fan type, size, and model of heat sink for electronics cooling. Also, another important conclusion drawn from this project is the existence of no definite correlation between the thermal resistance (R) and pressure drop (ΔP) parameters when evaluating heatsink performance.

CHAPTER 1: INTRODUCTION

Technological improvements over the years have led to the tremendous decrease in the size of electronic devices, hence leading to a higher heat flux generation. Due to this change, heat transfer or thermal management in these devices has become critical in the engineering and manufacturing of electronic devices, especially computers. Lee et al. [1] in one of his numerous studies on electronic failure due to thermal energy discovered that failure rates of electronic components almost doubles when the junction temperature increases by 10^0C beyond operating temperature.

Over the years, heat sinks have proven to be a viable thermal management device with a few open source information available on its optimum design. Plate-fin heatsinks are widely used to remove heat from electronic devices because of their advantages such as simple machining, structure and lower cost [2]. Main factors to consider in the design of heat sinks include a large heat transfer rate, low-pressure drop, and a simpler structure [3]. The goal of optimizing heat sinks is to decrease thermal resistance and minimize manufacturing and operational cost so as to meet operational requirements. Minimizing pressure drop and weight also affects the cost of operation since fan size and type is dependent on this parameter.

Factors that affect the performance of heat sinks mainly are:

- Air velocity
- Material

- Heat sink surface treatment
- Extrusion fin design (Geometry)

Commercial CFD software packages like ANSYS-FLUENT [4] and STARCCM+ [5] have become widely used in the thermal analysis and study of electronic devices due to their internally built heat transfer handling capability. Heat sink fin extrusion geometry comes in two main types, the plate fin which runs across the whole base of the heat sink and pin fin, arranged or sectioned in a specific pattern across the heatsink base. One of the most common heat sink fin design is the rectangular plate fin. This is due to its easy CAD modeling and manufacturability.

Subramanyam and Crowe [6] concluded that CFD based approach provides good and well-detailed information on the performance of heat sinks. This encouraged and motivated the use of CFD STAR CCM+ for this research. Gupta et al. [7] worked on CFD and thermal analysis of rectangular plate fin and cylindrical pin fin heat sinks with a primary focus on temperature and heat flux distribution. The results of this work revealed that with the same dimensions and boundary conditions, the thermal resistance is lower for rectangular plate fins as compared to a cylindrical pin fin heat sink. This is as expected due to the larger heat transfer surface area (A) of the rectangular plate heat sink. Yu et al. [8] performed similar work and concluded that thermal resistance of plate-fin heat sinks is lower by approximately 30% than that of pin fin heat sinks with the same blowing velocity.

Most computers CPU rely on heat sinks of various forms and shapes to keep them thermally operational. An efficient and reliable CPU plays a huge role in a computer's performance, thereby impacting the capabilities of any system in which it is used. Ismail et al. [2] compared four different types of heat sink: the Pentium III and IV, AMD Athlon, and AMD Duron. Using Fluent 6.2 CFD software simulations results were obtained and compared to experimental results. It was concluded that total surface area and fin spacing significantly affects heat sink performance. Fin density (Number of fins) influences thermal performance of heat sinks since the flow path of the working fluid is affected by the layout of fins. Densely stacked fins can inhibit the flow of coolant to the center part of the heat sink, which tends to be the hottest area. On the other hand, fewer fins increase the space between fins, which eases the airflow path resulting in lower pressure drop but also provide less surface area for heat transfer. One significant conclusion from Mohan and Govindarajan study on thermal performance of heat sinks is the effect on heat transfer as fin number is varied in relation to fin height [3]. That study showed that the sensitivity to the number of fins decreases as fin height increases due to the larger flow space provided across the heat sink. Mohan and Govindarajan [3] demonstrated the existence of an optimal fin number and geometrical parameters for a specific purpose heat sink.

The literature review illuminated the need for open source information that could potentially serve as a numerical validation case for fellow researchers in this area of study. For this reason, a main goal of the current paper is to provide credible and valid simulation results for various heat sink geometries and the

effects of changing certain parameters to optimize it using CFD software STAR CCM+ [5]. Results obtained from the simulations ran are compared with published experimental data. Also, this paper provides researchers information on best practices to follow when running valid simulations on various heat sinks.

1.1. Modes of Heat Transfer

Heat is a form of energy, hence can be transferred from one medium to another to conserve it. As a result of the law of energy conservation, heat transfer or thermal energy is transferred from a higher thermal energy surface or object to a lower medium or object. Heat transfer occurs in different modes under different conditions. The three modes of heat transfer that exist include conduction, convection, and radiation.

1.2. Electronic Cooling

Electronic cooling over the years has become more important due to the increase in heat flux generated in electronic devices. All electronic devices generate heat during operation. For an efficient, fast, and reliable operation of these gadgets, cooling needs to take place in order to keep the temperature within devices acceptable for functionality.

Several methods of electronic cooling exist, the most widely used include heat pipes, heat sinks, and impinging jets.

1.3. Conduction Heat Transfer Method

Conduction mode of heat transfer takes place within a solid or at the interface where objects are in contact. In a solid material, heat is transferred

through conduction as a result of the vibration of atoms against one another within it without the material not necessarily moving as a whole. In heat sinks, conduction takes place in two different phases. First is the heat transfer through conduction between the object being cooled and the base or bottom surface of the heat sink. The second phase is conduction within the heat sink from its base to the extruded fins. Heat from the hot bottom base of the heat sink is conducted to the extruded fin for dispersion to its surroundings.

1.4. Convection Heat Transfer Method

Convection heat transfer is the transfer of heat as a result of the movement of a fluid (e.g. water, air etc.). Two main types of convection exist based on conditions and desired results. Natural convection is a form of heat transfer in which no external source (fan, blower, or pump) is needed to move the fluid being used. On the hand, forced convection makes use of an external source to move the fluid. Most heatsinks operate by means of forced convection. In most cases, a fan placed so as to direct air through the fins of the heat sink.

Different flow directions are used in forced convection. The two directions are; Side inlet, Side exit (SISE) and Top inlet, Side exit. The placement of the external fluid source usually depends on size restriction and heat sink geometry.

1.5. Radiation Heat Transfer Method

Radiation is a form heat transfer that exists as a result of electromagnetic waves or light emission. This mode of heat transfer does not require a medium like the other forms discussed. Heat sinks do not rely on the radiation mode of heat transfer to function as a thermal management device. The dominant modes

of heat transfer in a heat sinks function are conduction and convection. These forms are present no matter what scenario or purpose a heat sink is used for.

1.6. Plate Fin Heat Sink

Plate-fin heat sinks as implied by their name are heat sink geometries that have their extruded fins running across the entire length of the base in the form of a plate. These types of heat sinks are the most commonly used in electronic devices. Heat sinks with plate fins can be modeled in different shapes and can also be arranged in different forms to force the direction of flow. Plate-fin heat sinks usually cover a larger surface area across the base of the heat sink. Hence, generally has a larger area for heat transfer since there's an increase contact area between the working fluid(air) and the material surface.

1.7. Pin Fin Heat Sink

Heat sinks with pin fin extrusions are widely used based on the ability to increase their surface area through the increase in the number of pins. Pin fin extrusions are usually layered across the base of a heat sink in a specified order or pattern so as to enhance airflow. One advantage of using pin fins over plate fins is that the direction of flow does not necessarily need to be precisely defined since all sides could work as an inlet though or outlet. In most cases depending on geometry, there is a direction of flow inlet and outlet that increase the performance of the pin fin heat sink and should be taken into account when mounted on the object to be cooled [9].

1.8. Exotic Geometry Heat Sink

With improved methods of manufacturing, manufacturers and researchers are able to manufacture objects of different shapes and dimensions. With geometry being a factor that affects the performance of heat sinks, the ability to manufacture heat sinks of different exotic geometries enables both thermal engineering and researchers to optimize heat sinks based on geometry modification. In this study, different heatsink geometries are analyzed under the same conditions and compared to each other based on their thermal performance and cost of operation. The exotic geometries in this study were modeled based on knowledge from fluid dynamics and heat transfer to better improve heat sink performance.

CHAPTER 2: LITERATURE REVIEW

In this chapter, studies conducted by other researchers over the years in this area of study is analyzed, and their contributions to the improvement and understanding of the heat transfer process in heat sinks is studied. With the knowledge gained from previous researchers work, the study done in this thesis project is aimed at adding more knowledge on heat sinks and solving potential problems or questions not answered by the literature available on heat sinks.

The continual development of electronic devices such as computers and its growing use in our day-to-day lives has made it eminent to focus on keeping them efficient and reliable. In an effort to improve functionality, reliability, and aesthetics, electronic devices have decreased in size tremendously and have become faster [7].

Many thermal management devices exist, one of the commonly used is the heat pipe. Heat pipes just like heat sinks are heat transfer devices used as a means of regulating the temperature in a system or machine for safe and efficient operation. Heat pipes are basically heat transfer devices that use the phase change within its working fluid to transport heat from a hot object. Key components of a heat pipe include a vacuum-tight sealed chamber, capillary wick structure, and a working fluid. The phase changes that occur during the heat transfer process in a heat pipe are evaporation and condensation. The evaporation process involves the conversion of the liquid working fluid into a vapor. The energy (sensible heat) used in this conversion process is obtained from the ambient air around the heat pipe. The reverse case (condensation) then occurs as the hotter fluid vapor(gas)

is transferred to the cooler part of the pipe where heat is dispersed. Therefore, the heat transfer process within a heat pipe can be separated into two different sections, the heat source (evaporator section) and heat sink (condenser section) [10].

The most common thermal management device for electronic cooling is the heat sink. Heat sinks work just like radiators in cars, they regulate the temperature in the machine or device in which they are installed to keep them operationally safe.

Ismail and Abdullah [2] compared four different types of heat sinks: the Pentium III and IV, AMD Athlon, and AMD Duron heat sinks. Fluent 6.2 computational fluid dynamics software was used in running simulations and results obtained were compared to experimental results. The flow and temperature fields of the heat sink at different Reynolds numbers were analyzed and results showed that the thermal impedance ($\ominus$) reduces as Reynolds number increases (Re_L). The thermal impedance is based on the temperature difference between the surrounding temperature and the base surface temperature of the heat sink.

$$Re_L = \frac{V_\infty L}{v} \quad \text{.....Equation (1)}$$

$$\ominus = \frac{T_{base} - T_\infty}{Q} \quad \text{..... Equation (2)}$$

In Ismail and Abdullah's work, it was also deduced that larger fin spacing results in better heatsink performance [2]. Also, experiments run by Ismail and Abdullah proved that higher surface area and suitable fin density provide better heat sink performance. In conclusion, the Pentium IV heat sink was determined to give the best thermal management in comparison to the AMD Athlon and

Duron.

Korpys [11] investigated the performance of a commercial heat sink fixed to the CPU of a PC using water and copper oxide (II) nanofluids as working fluids. The heat sink was used in cooling the processor of the computer that dissipated 115W of power. The performance of water and copper oxide (II) nanofluids was analyzed using experimental and simulation methods. Results obtained showed that the simulation and experimental approach produced similar results in relation to the cooling of the PC ‘s processor. Water was determined to be a good enough coolant for a CPU.

Majumber et al. [12] studied the cooling performance of a heat sink with air-water flow through a mini-channel. In their study water flows internally through the mini-channel fins of the heat sink while air flows externally. It was observed that as the aspect ratio (height/width) of the channel decreases the Nusselt number decreases while pressure drop increases. Nusselt number is observed as directly related to the Reynolds number hence the Reynolds number increase results in an increase in Nusselt number as well.

Matthew B. de Stadler [13] studied a similar research on optimizing the geometry of heat sink by determining an optimal layout for a given heat sink. In his work, his goal was to determine a valid performance metric for ranking different designs of a heat sink. Boundary conditions used in this research were set at a constant surface temperature, which resulted in inconsistencies of results. This research paper showed that there are difficulties in using fixed temperature boundary condition for the hot base plate since no significant results were

obtained from simulations run. Future works recommended by Stadler include running simulations using a constant heat flux boundary condition.

Gupta et al. [7] worked on CFD and thermal analysis of rectangular plate fin and cylindrical pin fin heat sinks with a primary focus on temperature and heat flux distribution. The results of this work showed that with the same dimensions and boundary conditions total heat transfer rate of rectangular plate fins are greater than cylindrical pin fins as expected.

Subramanyam et al [6] to investigate ways of rapidly designing heat sinks using computational and experimental tools. He discovered that CFD based approach though costlier provides better and more detailed information and predicts the performance well. This encouraged and motivated the use of CFD STAR CCM+ for this research.

In a study by Seri Lee [14], the relative cost associated with varying parameters that affect heat sink performance was analyzed for optimization purposes. Conclusions drawn from this research showed that there are an optimum fin length and number for specific heat sink designs to obtain optimum performance. Experimental results from Dogan and Sivrioglu's [15] study on mixed convection heat transfer from plate-fin heat sinks inside a horizontal channel in a natural convection region also supported this conclusion.

Above a certain point (number of fins), the net effect of thermal performance reverses due to total convective surface increase resulting in greater pressure drop hence fin flow velocity decreases as well. The same can be said for fin lengths exceeding optimum point due to temperature rise in the air stream

between fin surfaces in conjunction with a reduction in flow velocity increasing the pressure drop.

The determined optimum fin spacing range for heatsinks is between 8-12mm [15].

Zheng and Wirtz [16] studied heat transfer and pressure drop correlation in a pin-fin fan heat sink and came to the same conclusion as Seri Lee [14] from his study. Their work showed that different optimal pin-fin configurations provide different results depending on the design criteria imposed on the flow.

Lindstedt et al [17] investigated the optimal shape of single fin and fin array heat sinks. He considered three different heat sink geometries: rectangular, triangular, and trapezoidal. It was found that due to the coupling of convection and conduction, the most concave geometry i.e. triangular explicitly serves as the optimal single fin heat sink geometry. On the other hand, with fin array heat sinks, trapezoidal fins were determined to give the best practical compromise for thermal resistance, fan power, and mass proving that optimal shapes of single fin heat sinks cannot be used to optimized fin arrays in heat sinks.

Mini channel heat sinks have been proven to be viable methods of thermal management. Majumder et al. [12] worked 3-Dimensional numerical study of cooling performance of a heat sink with air-water flow through mini-channel.

Impinging jets perform a similar function as heat sinks but mostly on larger scaled objects or devices. The jet impingement cooling technique produces relatively higher heat and mass transfer in comparison to other methods used [18].

Rocket launchers and turbine blades implement different forms of impinging jet layouts for cooling during operations. Like the heat sink extruded fins, the arrangement of jets in the impinging jet affects thermal performance of these cooling devices or techniques.

Different fluids such as coolants used in refrigerators ensure good thermal energy transfer from heat sinks to air. Fans used in conjunction with heat sinks also helps improve heat transfer between heat sinks and surrounding air. Using air as a means of cooling electronic devices is an important technique in designing these devices for various reasons including it being readily available, safe, the process does not cause any form of contamination to the air, does not incorporate vibration, noise or moisture to the system being used [19].

For example, Lampio and Karvinen [20] generated a method to calculate the temperature field and heat transfer of a heat sink cooled by forced or natural convection(air).

Surrounding conditions or the system within which a heat sink operates affects its thermal performance. Depending on the location of the heat sink and the surface area the heat source device covers on the bottom surface of the heat sink base, thermal energy distribution may vary within the heat sink. For this reason, an advanced simulation work was conducted by Mohan and Govindarajan [21] on thermal analysis of composite pin fin heat sinks in a complete computer chassis. This study ensured the simulation of environmental condition effects on heat sink thermal performance during operation. Figure 1 below shows a schematic of the complete computer chassis studied.

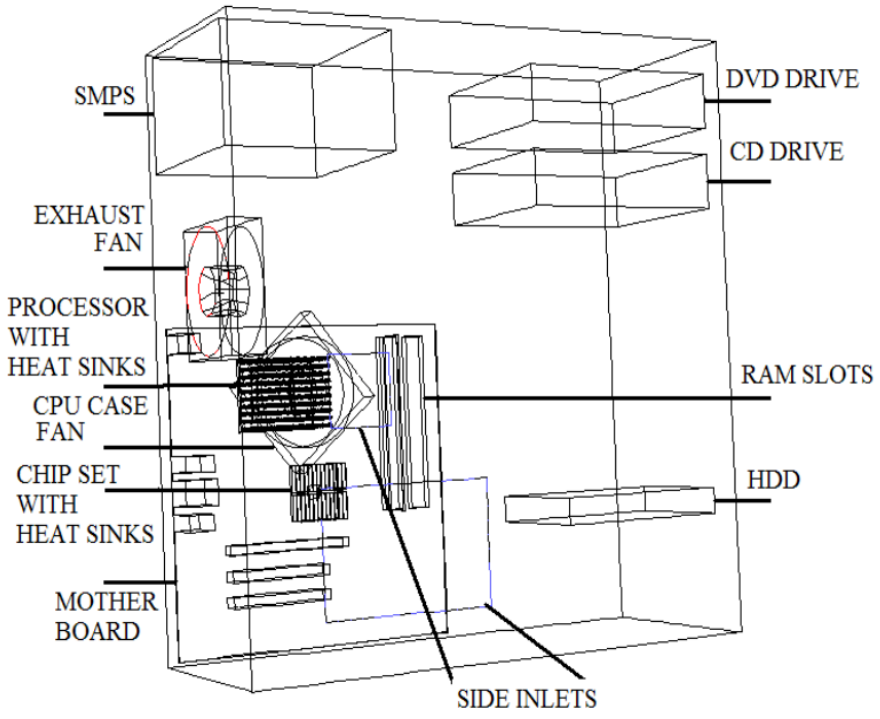

Figure 1: Full computer chassis model [21].

The computer chassis and component locations were kept constant while heat sink designs were changed for the simulations conducted. Velocity field and flow path around heat sink were affected by the presence of other components involved in their study. Hot air flow recirculation can be reduced by using plate-fin heat sinks instead of pin fin heat sinks in some situations.

The weight parameter also is very important when designing heat sinks for various purposes. Usually, devices in which heat sinks are installed have weight limits or are desirable when lightweight. For this reason, optimizing the weight of a heatsink is an area of focus when design engineers work on improving electronic devices as a whole. Optimizing this parameter also reduces the cost of

manufacturing of these heatsink models. One approach in reducing weight is creating channel holes through fins of heat sinks, this not only reduces weight but also allows designers to model air flow paths for better heat transfer since these holes function as a channel for air flow through and around heat sink fins [22]. Sukumar et al. [22] studied a continuous and interrupted rectangular fin heat sink geometry performance with and without through holes. From results obtained, the through holes heat sink for the interrupted fins performs better than the interrupted fin without holes. This conclusion is interesting since an increase in surface area is expected in most cases to increase heat transfer performance of the heat sink.

Another growing but more complex research area on the optimization of heat sink designs is the use of topology [23]. This form of design optimization utilizes objective functions to optimize a specific desired parameter that affects heat sink performance (thermal resistance, pressure drop, weight). Topology optimization provides a faster mode of generating design concepts but manufacturability is not always guaranteed as some of the geometries the functions produce are very complex. To achieve feasible manufacturability of topology optimized heatsink designs, fabrication constraints can be set up in the optimization process.

For this reason, Wits et al [24] in his study utilized 3D printing/additive manufacturing method in manufacturing complex objects from different materials. The 3D printing or additive manufacturing process is a more modern way of creating three-dimensional objects by the additions of layers using

computational control.

2.1. Microchannel Heat Sinks

A microchannel heatsink is a heatsink with microchannel extrusions incorporated with the intended purpose of improving heat transfer by allowing the working fluid flow within it. The concept of microchannel heat sinks was introduced in 1981 by Tuckerman and Pease [25] as a means of heat transfer in electronic devices. Just like normal heat sinks without microchannels, the performance of microchannel heat sinks is affected by size and shape.

Zhang et al. [26] researched the effects of the channel shape on the cooling performance of the hybrid microchannel and slot-jet heatsink module. A study on new hybrid jet impingement/microchannel cooling scheme by Barrau et al. [27] proved the success of improving cooling performance through the use of hybrid jets and microchannels.

Chen et al [28] looked into three-dimensional simulations of heat and fluid flow in noncircular microchannel heat sinks. This was done by creating triangular, rectangular, and trapezoidal shaped microchannels through the heat sink geometries simulated. From their work, the conclusion was drawn that a triangular microchannel provides a higher cooling efficiency than a rectangular and trapezoidal channel.

Lee and Garimella [29] studied heat transfer in rectangular microchannels of different aspect ratios and found that for a rectangular microchannel heatsink, a higher aspect ratio does not necessarily increase but can also decrease its thermal resistance. Figure 2 below shows a schematic of a microchannel heat sink.

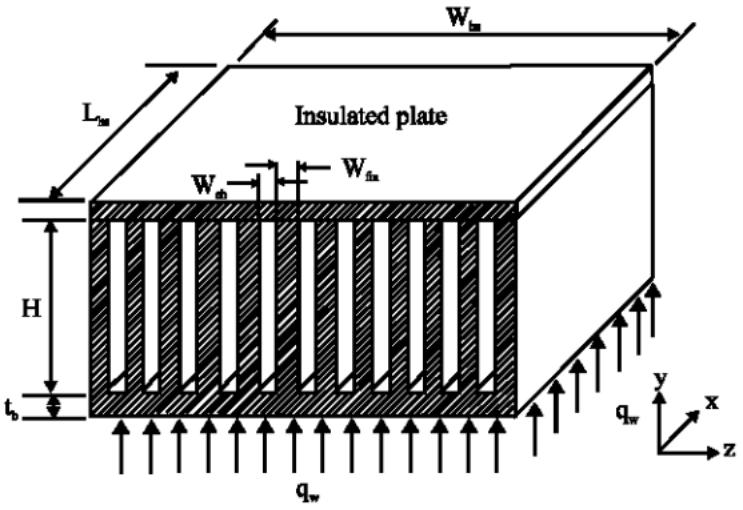

Figure 2: Schematic diagram of a microchannel heat sink [30].

In addition to the introduction of microchannels to improve the heat transfer of heatsinks, researchers over the years have studied the effect of various geometry modifications on the performance of heat sinks.

The two most traditional cooling techniques and modifications incorporated mostly in electronics cooling are micro-channel flow and impinging jets [31].

Huang et al. [32] studied heat transfer enhancement of a micro-channel heatsink with impinging jets and dimples. This was done by comparing different dimple structures including concave, convex, and mixed dimples to no dimples on a microchannel heatsink. It was determined that micro-channel heatsinks with convex dimples exhibited the best cooling performance followed closely by micro-channel heatsinks without dimples, then mixed dimples and concave dimples.

Similarly, Barik et al. [33] researched heat transfer enhancement using

different surface protrusions in a rectangular channel.

As part of the desire to improve upon the traditional plate-fin heat sink design so as to enhance its performance, the cross-fin heat sink design shown in Figure 3(b) below has been noted to improve the overall (natural convection and radiation) and convective (excluding radiation) heat transfer coefficients by 11% and 15% respectively [34].

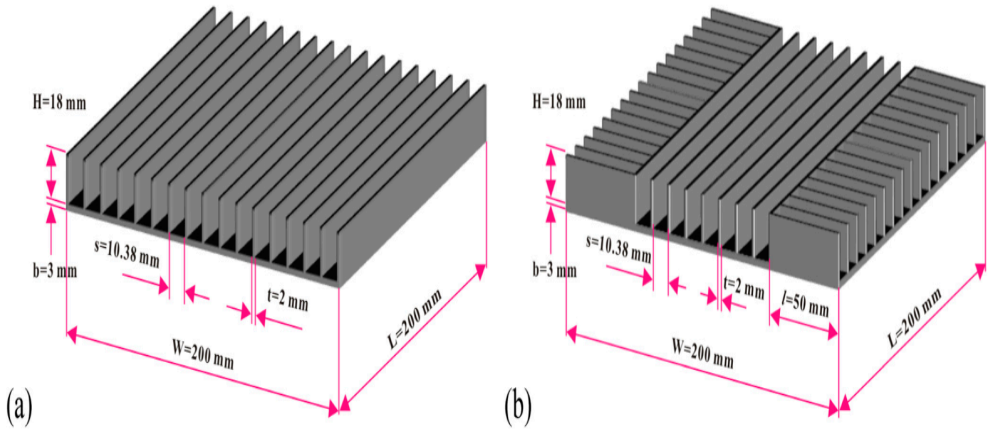

Figure 3: Schematic of (a) Traditional plate-fin heatsink and (b) cross-fin heatsink [34].

Ledezma and Bejan [35] proposed in their work that slope plate-fins enhance heat transfer for natural convection in heatsinks. Kim [36] similarly studied the thermal optimization of plate-fin heat sinks under natural convection by varying its fin thickness.

Elshafei [37] concluded that hollow circular pin fins possess a better natural convective heat transfer performance than fully solid extruded pin fins without any modifications.

Considerations in Heatsink design

Different factors are known to affect heat sink performance, hence the existence of various ways to evaluate their performance. In Karimpourian et al. [38] work, the following observations were made about heatsink performance and the performance evaluation parameters for heat sinks were listed as follows:

- Thermal resistance; which is a characteristic of the heat sink.
- The measure of maximum temperature rise of the heat sink or base against pressure drop.
- For a single active heat sink, pressure drop versus fan rotational speed can be used to determine heat sink performance.

Designing fin arrays in a heat sink can be complex because of performance variables producing opposite effects [19]. Variables such as the location of heat generating components, number of fins, fin geometry, the volume of the array, and pump or fan power used may affect heat sink performance directly or indirectly depending on the variable being optimized.

Though solving for performance results can be complex and time-consuming analytically, some methods are available to solve these problems for reasonable results [17].

With the various limitations and difficulties involved in the use of the analytical method in the optimization process, researchers in heat sink optimization usually employ numerical analysis as a means of testing heat sinks. This method allows the handling of complex equations, multi-variable functions, and problems the human brain would have difficulty in solving.

2.2. Key findings from Literature Review Conducted

From the literature review conducted some of the key findings relevant to this research project include:

- Different fin geometries and dimensions affect the thermal performance of heat sinks. e.g. microchannel.
- A Goldilocks region exists in the design of heat sinks; at this point, the possible maximum or optimum performance of a heat sink is obtained.
- Thermal resistance and Pressure drop are effective ways to evaluate the performance of a heat sink.
- External conditions such as working fluid used in heat sink operation affect the performance of a heat sink.
- The use of CFD tools is a viable and credible method of testing heat sink performance.

2.3. Research Objective

The literature review conducted illuminated the need for open source information that could potentially serve as a numerical validation case for fellow researchers in this area of study. For this reason, the main goal of this research project is to provide credible and valid performance simulation results for various heat sink geometries and the effects of changing certain design parameters to optimize heat sinks using numerical CFD simulation. Results obtained from the simulations ran are compared with published experimental data for validation. An

optimization case is established by improving upon the widely used traditional plate-fin heat sink geometry by comparing its performance to that of other generated geometries.

Also, this research provides researchers information on best practices to follow when running numerical simulations on heat sinks.

CHAPTER 3: METHOD AND APPROACH

Methods and techniques used in the generation and simulation of heat sink CAD models and CFD analysis are discussed in this chapter. Best practices and relevant parameters adopted in simulating various geometry heat sinks using CFD tool STARCCM+ [5] is also discussed in this chapter. The physics behind modeling real-world conditions for the accuracy of results is explained based on the models selected for the type of heat sink analyzed.

3.1. Methodology

3.1.1. Conjugate Heat Transfer Method (CHT)

The existence of a solid and fluid region in this study made it relevant to implement the conjugate heat transfer method in simulating the models. This method allows for the modeling of both heat sink (solid) and the air (fluid) physics and their interaction between each other at their interface. Within the heat sink device, conduction heat transfer method dominates since the thermal energy is transferred from the hot base to the other areas of the heat sink as a result of the interaction or collision between the internal molecules within the material (aluminum).

Convection heat transfer dominates in the fluid region. This heat transfer is important in this simulation work since it depicts the effect of heat transfer between the heat sink and its surroundings (ambient air).

3.2. Fluid Modeling

In order to ensure the validity of the results compared to the different heat sink geometry simulations run, assumptions were made so at replicate real-life behavior of fluid(air) flow around heat sinks. As stated above, the conjugate heat transfer method was used in this study, hence the existence of the solid and fluid regime. The fluid properties and its volume occupied were kept constant for all the heat sink simulations run.

The fluid flow was modeled to stay in the laminar region. Laminar flow corresponds to smooth fluid flow with little to no form of disturbance. This type of flow moves in a regular path and is assumed to possess a much steadier velocity and pressure drop. Flow properties in laminar flow are also assumed to be constant across its path of flow. Due to the conditions under which the heatsink tested in this project are to be used, the laminar flow model was deemed appropriate since fluid movement is relatively slow, and the flow channel is relatively small.

The segregated fluid temperature model is used in scenarios where fluid temperature is considered independent of the solid under a conjugate heat transfer method. This model solves the energy equation with variant independent temperature [39].

3.3. Reynolds Number

Reynolds number is a dimensionless quantity used in describing flow in or around a system. Whether a fluid flow is laminar or turbulent can be determined by the value of its Reynolds number using the formula:

$$Re = \frac{\rho \bullet V \bullet D_h}{\mu} \quad \text{.....Equation (3)}$$

$$D_h = \frac{4 \bullet A}{P} \quad \text{.....Equation (4)}$$

This formula basically reflects the ratio of the inertial to viscous forces and predicts flow behavior based on the two different flow regimes stated (laminar and turbulent). The laminar flow which is a slower steadier flow occurs at a low Reynolds number of less the 2,300. Between a Reynolds number range of 2,300 to 4,000 the transition between laminar and turbulence begins to occur. At this state, both laminar and turbulence flow regime coexist, hence a fluid in this state possesses properties of both laminar and turbulent flow. After a Reynolds number of 4,000 the turbulent regime is reached. In this regime, the flow is unstable due to a more dominant inertia force creating more disturbance within the flow.

From Equation 3, it can be deduced that in a study like this were fluid type is kept constant, the parameters ρ, ν, and μ remains relatively the same for different model heatsink testing. With the geometry diameter (D) kept constant as in the case of the geometries studied, the driving parameter of the Reynolds number is the velocity change. Hence, leading to the selection of a constant velocity of (1m/s) being used as the approaching airflow velocity across the heat sinks. As stated earlier, the flow in the simulations run were all kept within the laminar flow region at a value of 1,150.

This allowed for the acquisition of more realistic results since most of the fans used in driving air flow velocity across heat sinks mostly are not capable of generating turbulent flow at the required higher fan speed.

3.4. Governing Equations

The governing equations for fluid flow mechanics used in this study represent the numerical expressions for predicting the behavior of the fluid around the heat sinks simulated. Fluid motion equations are typically very complex in nature and mostly require computational power and skills for better and accurate prediction results. In cases like this were fluid behavior around and within a 3-dimensional object is desired, solving the continuity equations for fluids becomes very tasking due to the different dimension needed to be considered.

The equations built into the computational software (STARCCM+) used in this study is the Navier-stokes equation. This equation is derived from Newton's second law when applied to fluids in motion under stresses. The stresses from which the Navier-stokes equation is derived from is as a result of the combination of the diffusion viscous term and pressure. A vector form of the Navier-stokes equation is shown below:

$$\frac{\partial \rho}{\partial t} + \nabla \cdot (\rho \boldsymbol{u}) = 0 \quad \text{.....Equation (5)}$$

$$\frac{\partial \boldsymbol{u}}{\partial t} + (\boldsymbol{u} \cdot \nabla)\boldsymbol{u} = -\frac{1}{\rho}\nabla \rho + F + \frac{\mu}{\rho}\nabla^2 \boldsymbol{u} \quad \text{.....Equation (6)}$$

$$\rho\left(\frac{\partial \varepsilon}{\partial t} + \boldsymbol{u} \cdot \nabla \varepsilon\right) - \nabla \cdot (K_H \nabla T) + \rho \nabla \cdot \boldsymbol{u} = 0 \quad \text{.....Equation (7)}$$

$$\text{where } \nabla( ) = \mathbf{i}\frac{\partial}{\partial x} + \mathbf{j}\frac{\partial}{\partial y} + \mathbf{k}\frac{\partial}{\partial z} \quad \text{.....Equation (8)}$$

3.5. Flow-through heat sink fins

The flow path through extruded fin heat sinks plays a major role in the removal of heat across its surface area. Different fin arrangements can be generated for both pin and plate heat sinks to enhance heat transfer. The distance between fins, height, and width of fins are important specifications when considering flow through fins. In this study and for simulation purposes, steps were taken to maximize the flow through the heat sink fins so as to generate optimal heat transfer from the heat sink surface to the working fluid.

3.6. CAD Model Generation

For the CAD modeling of the heat sinks studied for this thesis, Solidworks [40] was used. The generation of the model can be separated into two different parts: the base and extruded fins which are the main parts of the heat sink.

First, a sketch of the heat sink base was generated and extruded to form its thickness. Dimensions and shape of the base can be seen in Figure 4.

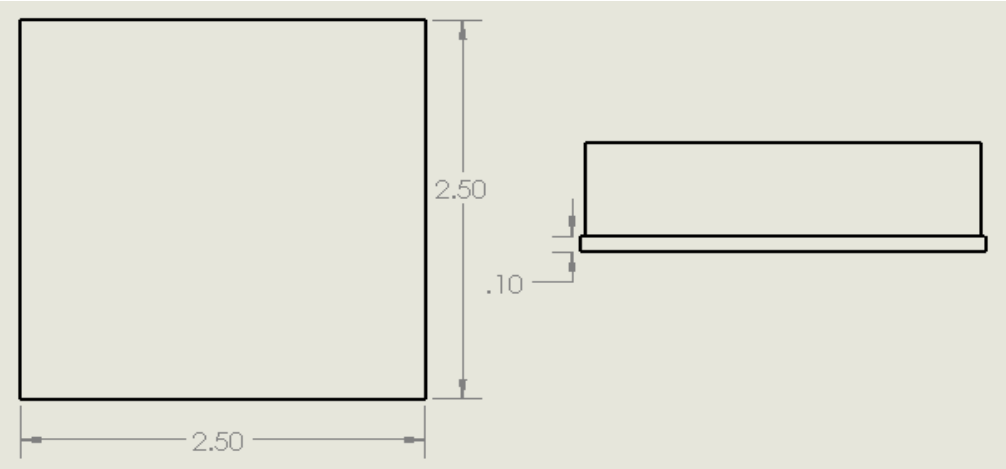

Figure 4: Heatsink base dimensions in inches.

Next, a sketch of the pin or plate fins was generated across the base of the heat sink and extruded. For faster and simple modeling of the extruded fin ones, one sketch was created and extruded the linear pattern function was used to create the number of pin or plate fins desired. This parameter was also kept constant in all the heat sink models generated for better comparison results. For the pin fin heat sinks, the fins were arranged in a 13 X 25 matrix order while the plate fin heat sinks had 25 fins. Figures 5 (a) and (b) shows an image of the plate and pin fin heat sinks and their fin arrangements respectively.

In order to ensure the accuracy of heat sink performance results obtained and compared, the dimensions for the base and extruded fin height and width (diameter) were kept constant for the differently shaped heat sink designed generated.

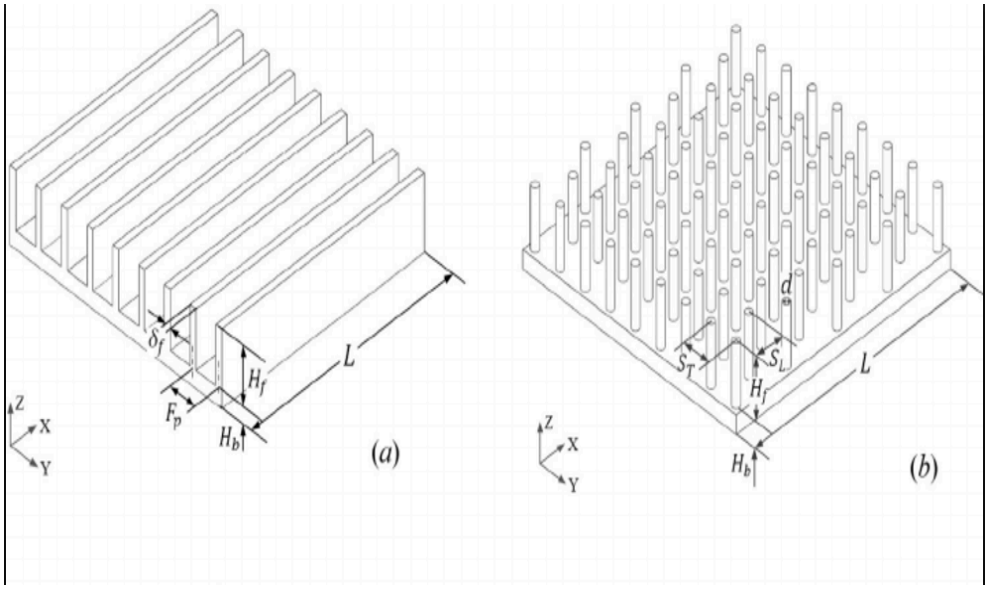

Figure 5: Schematic of (a) Plate fin heatsink (b) Cylindrical Pin fin heatsink.

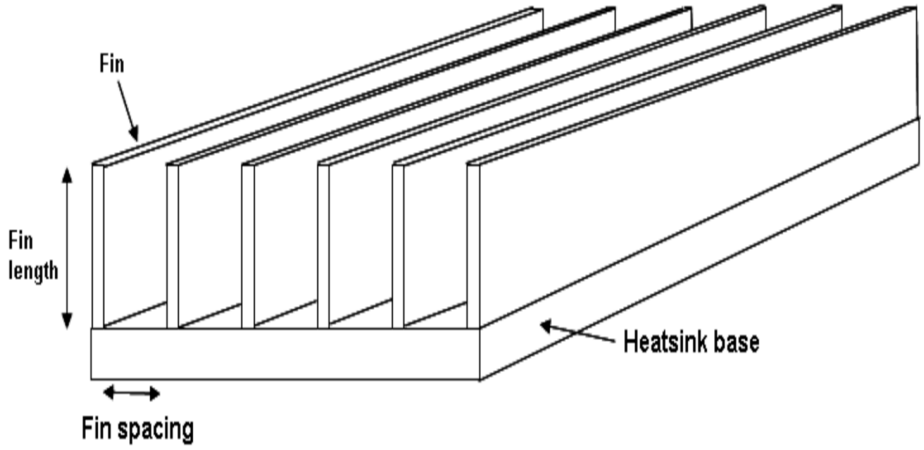

Figure 6: Schematic of Plate fin heatsink with labeled part [41].

3.7. Validation Case

To start this study, a validation case was established based on the literature review conducted to ensure results obtained from the simulation run were accurate and the assumptions and models used were valid. Using experimental results from Loh and Chou's [42] work on the comparative analysis of heat sink pressure drop using different methodologies, a validation case was established. In their work, a theoretical, experimental, and numerical study was done and compared to each other for validation. For the theoretical method, three equations for solving pressure drop were derived from the force balance on the heat sink and the Flemings and Darcy equations. Below are the equations generated:

$$\Delta P = \left(\frac{f_{app} \cdot N(2HL+bL)}{HW} + K_c + K_e\right)\left(\frac{1}{2}\rho V_{ch}^2\right) \quad \text{.....Equation (9)}$$

$$\Delta P = (4f_{app}x^+ + K_c + K_e)(\tfrac{1}{2}\rho V_{ch}^2) \quad \text{.....Equation (10)}$$

$$\Delta P = 4(f_{app}x^{+} + K_c + K_e)(\frac{1}{2}\rho V_{ch}^2)$$ …….. Equation (11)

Two different equations for the channel velocity (V_{ch}) were input into the ΔP equations above and compared to each other as well.

$$V_{ch} = V_{ap}(1 + \frac{t_f}{b})$$ ……..Equation (12)

$$V_{ch} = V_{ap}(\frac{A_f}{A_{tf}})$$……...Equation (13)

After comparing results, a combination of Equations (5) and (1) were determined to be the most accurate in calculating the theoretical pressure drop.

The experimental setup in this study as stated was used as the basis for establishing a validation case for this thesis work. The heat sink geometry tested was a rectangular plate with geometry specifications shown in Table 1 and Figure 8. A controlled wind tunnel test section presented in Figure 10 was used in analyzing the pressure drop across the heat sink geometry testing. In order to prevent any flow bypass, the heat sink was fully ducted on the top and both sides. This made it possible to measure the actual maximum pressure drop through the extruded fins of the heatsink. The experimental test was conducted at an air velocity range of 1m/s to 4m/s with 0.5 increments. Figure 7 below shows a plot of the experimental, numerical (Flotherm), and analytical test results at varying approaching air velocity.

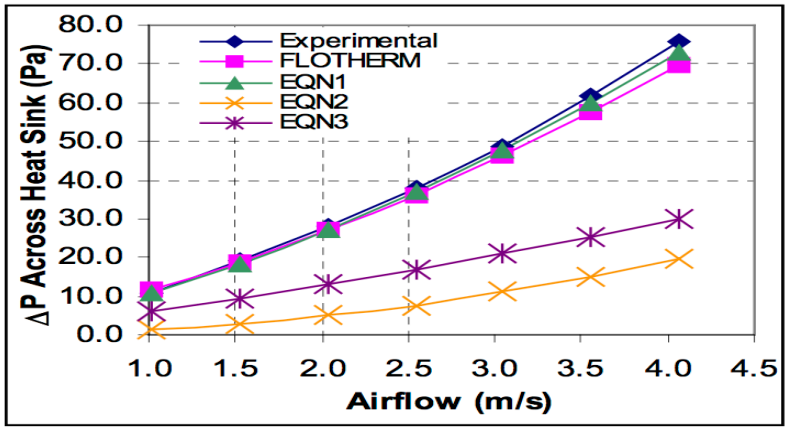

Figure 7: Validation case heatsink results [42].

The numerical analysis was performed using FLOTHERM v4.1 [43] and both heat sink and wind tunnel test section was modeled after the experimental setup discussed.

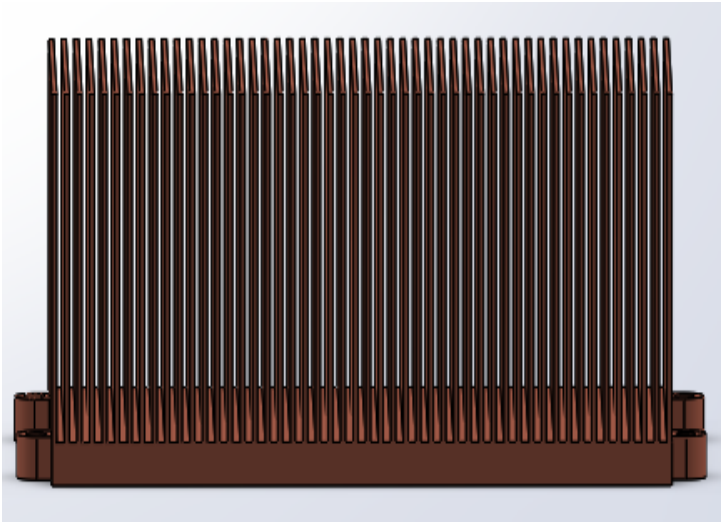

Figure 8: Validation case heatsink CAD model.

Table 1: Validation Case Heatsink geometry specifications [42].

Test Sample	Validation Case Heat Sink
Width (W)	126 mm
Length (L)	75 mm
Height (H)	63 mm
Fin Thickness (t)	1 mm
Channel Width (g)	1.55 mm
Base Thickness (b)	7 mm

As stated in earlier sections, active heatsinks rely on a fan or some sort of fluid driving device to function. Since a well-defined airflow path (inlet) is modeled in this study, the heatsink tested are active heatsink with a specific inlet flow direction like the example in Figure 9.

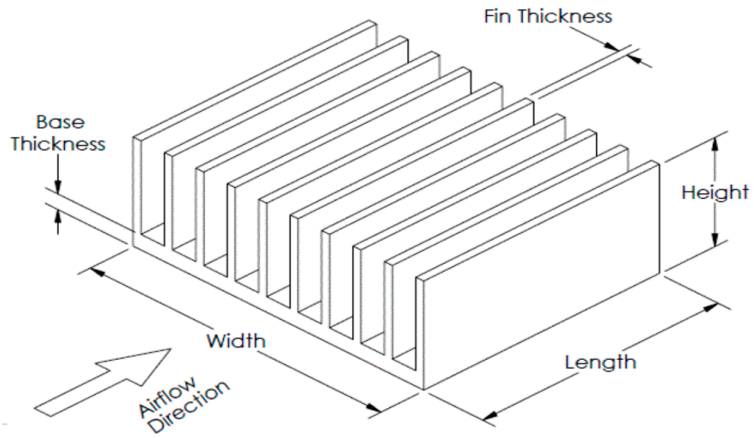

Figure 9: Schematic of an Active heatsink with flow direction [44].

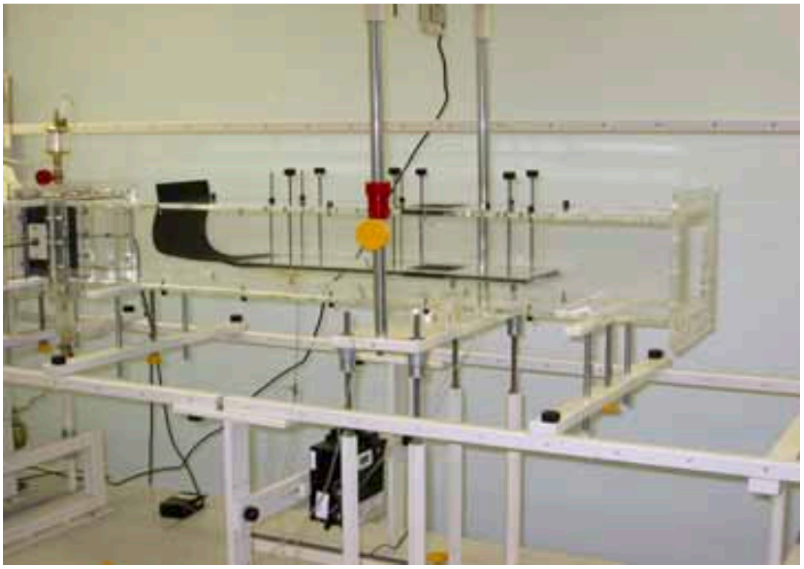

Figure 10: Experimental case wind tunnel test section [42].

3.7.1. STARCCM+ Simulation of Validation Case Heatsink.

The simulation approach used in this study as explained in earlier chapters is the conjugate heat transfer method. Hence the modeling and simulation of the validation case and the various geometry heat sink designs analyzed can be separated into a solid and fluid domain.

For the validation case, the heatsink CAD model in Figure 8 above was generated in Solidworks using the model dimension specifications from Table 1. This model was then imported into STARCCM+ for simulating. With the heat sink which represents the solid domain imported, the fluid domain was then created around the heat sink (solid domain). In order to correctly replicate the experimental setup, the fluid domain was modeled to make direct contact with the sides and top of the heat sink so as to prevent any flow bypass as seen in Figure 11.

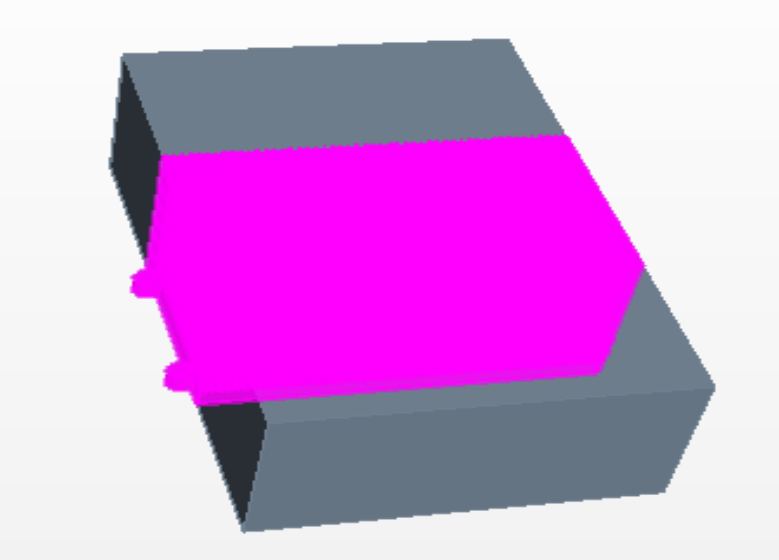

Figure 11: Representation of solid and fluid region of the simulation model.

Next, the meshing and physics models were selected to replicate experimental conditions. Different physics models were selected for the fluid and solid regions since both require different assumptions to be correctly modeled. Tables 2, 3, and 4 below lists the selected meshing, and physics (fluid and solid) models for the validation case heat sink.

With the mesh generated to capture full heat sink geometry in STARCCM+, the simulation was then run to produce scalar scene plots of temperature distribution and pressure drop for results comparison between the various heat sinks analyzed.

For the validation case, the pressure drop results from the simulation run was compared to the experimental results from the literature review. The results and comparison details are presented in the results and discussion section.

Table 2: Meshing Models.

Enabled Models
Advancing Layer Mesher
Extruder
Surface Remesher

Table 3: Fluid (Air) Physics Model.

Fluid Enabled Models
Gravity
Segregated Fluid Temperature
Ideal Gas
Laminar
Gradients
Segregated Flow
Gas
Steady
Three Dimensional

Table 4: Solid (Heat sink) Physics Models.

Solid Enabled Models
Constant Density
Gradients
Segregated Solid Energy
Solid
Steady
Three Dimensional

3.8. Heat Sink Simulations Generation and Assumptions

As discussed, the validation case established served as the blueprint for the simulations run on the various geometries tested. Hence the physics models (Fluid and solid models) used in generating similar experimental and validation case results were used in all the simulations run. However, it is important to note that the meshing models were changed due to geometry changes so as to capture the full geometry of the various heat sink geometries studied. For the heat sinks tested in this research project, the meshing, fluid, and solid models selected are presented in Tables 5, 6, and 7 below respectively.

Also, the ambient air or working fluid conditions were also kept constant to ensure the results obtained were fairly comparable. The velocity of the approaching fluid (air) at the inlet was kept at a constant 1m/s, the temperature at 300 K, and an atmospheric pressure of 101,325 Pa. With the simulation run to 1,000 iterations, scalar scene results were generated for the temperature and pressure profile. This was then used in calculating the thermal

resistance and pressure drop respectively to compare the performance of the heat sinks simulated.

Table 5: Simulated Heatsink Meshing Models.

Enabled Models
Embedded Thin Mesher
Extruder
Generalized Cylinder
Polyhedral Mesher
Surface Remesher

Table 6: Simulated Heatsink Fluid (Air) Physics Models.

Fluid Enabled Models
Gravity
Segregated Fluid Temperature
Ideal Gas
Laminar
Gradients
Segregated Flow
Gas
Steady
Three Dimensional

Table 7: Simulated Solid (Heatsink) Physics Models.

Solid Enabled Models
Constant Density
Gradients
Segregated Solid Energy
Solid
Steady
Three Dimensional

3.9. Geometry Comparison

As mentioned earlier, in order to ensure results gained were actually comparable, constraints were set for the simulated heatsink geometry dimensions. Table 8 below gives a well-defined representation of the dimensions of all the heatsinks modeled and tested for in this study.

Table 8: Simulated Heatsink Geometry Specifications.

Test Sample	Simulated Heat Sink
Width (W)	63.5 mm
Length (L)	63.5 mm
Height (H)	18.3 mm
Fin Thickness (t)	1.27 mm
Channel Width (g)	2.54 mm
Base Thickness (b)	2.54 mm

It is important to note and understand that, though fin type and shape were changed, their thickness and channel width (distance between fins) were kept constant. This permitted results to be compared and analyzed based on enhancement of heat sink fin geometry.

3.10. Method of Data Comparison and Analysis

To compare the various heatsink models generated in this study, bar graphs were created from tabulated simulation results representing the value of their corresponding performance evaluating parameters (thermal resistance and pressure drop). Two plots were created to compare thermal resistance and pressure drop of the modeled heatsinks. Analysis of results was then performed based on the height of bars associated with heatsink fin geometry model.

CHAPTER 4: RESULTS AND DISCUSSION

In this chapter, numerical results obtained from the simulations run in this study is presented and discussed.

4.1. Validation Results

The validation case simulation result for the heatsink model at a velocity of 1m/s discussed above is presented in Figure 12 below.

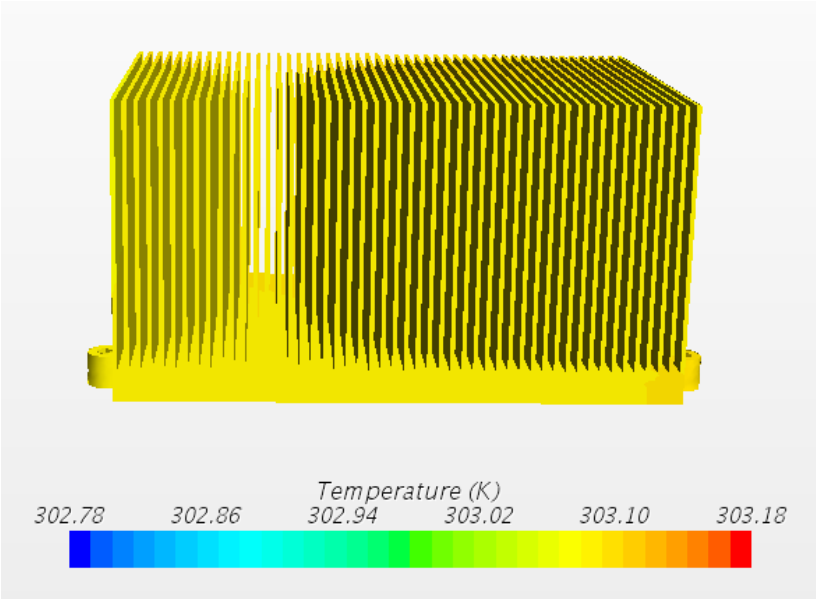

Figure 12: Validation case heatsink simulation.

A graph comparing the simulation and experimental results for the validation case heatsink was generated and presented in Figure 13. From this graph, it is observed that the experimental and simulation results are close with a mean absolute percent error (MAPE) of 8% and serves as a good validation case for simulating heatsink models in STARCCM+.

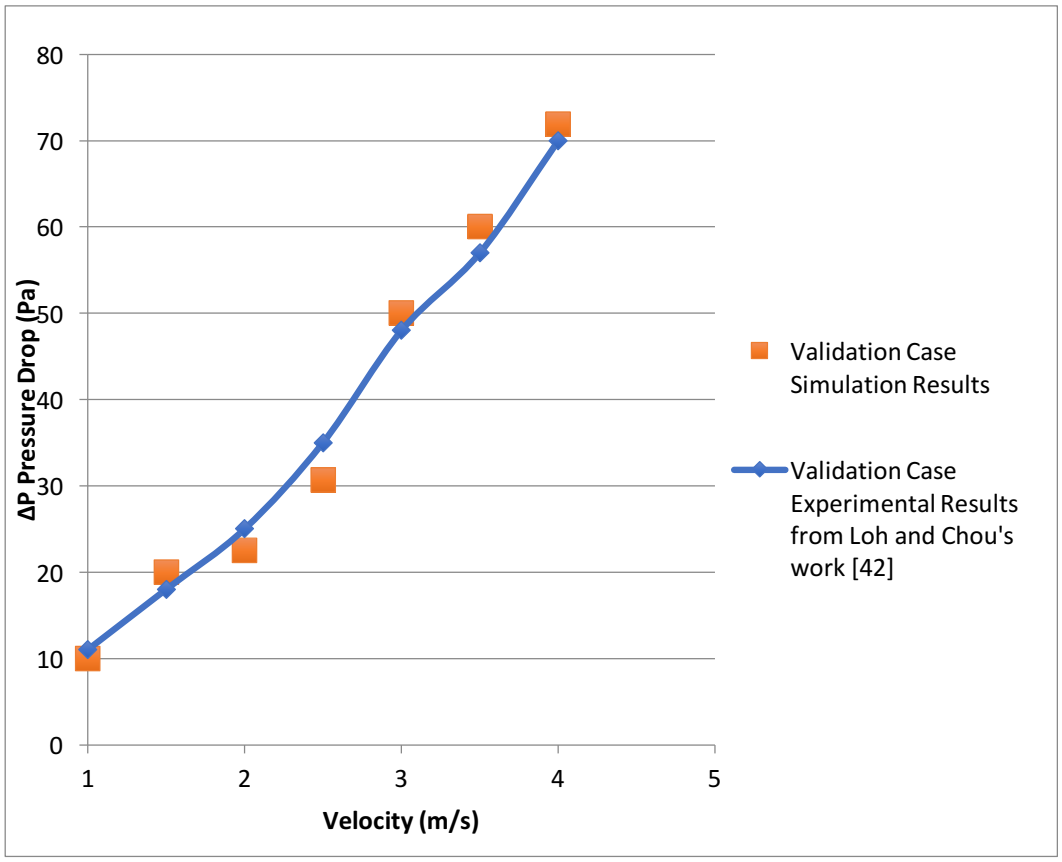

Figure 13: Graph comparing experimental and numerical data results.

From published literature and research conducted, several ideas for heatsink models with the potential to produce better results than the traditionally used rectangular heatsink was modeled and simulated. Also, models were generated using knowledge from fluid dynamics and heat transfer courses. Results from the simulations run are presented in the following sections.

4.1.1. Temperature Profile Results

Temperature profile results from simulations run are used in conjunction with the constant power supply (100W) in calculating the thermal resistance (R) of the heat sinks, Equation (14). The hottest temperature (T_{base}) is usually located at the base of the heat sink since it makes direct contact with the heat source. It is important to note that the spread of thermal energy is not uniform across the heat sink. Hot spots are generated in areas as a result of different factors including design and flow path.

$$R = \frac{T_{base} - T_{\infty}}{Q} \quad \text{..... Equation (14)}$$

In this section of this chapter, different heatsink geometries are studied for their temperature profile to determine performance. Figures below show the temperature profile of the heat sink during its operation (1000 iterations).

As expected and shown in scalar scene result figures below the fins located in the frontal section of the heat sink tend to have the lowest temperature. This is due to the fact that they are the first part to come in the contact with the cool air supplied by the fan or fluid supply source during its operation. On the other hand, the surface closest to the exit or farthest from the inlet possesses a higher temperature since flow moving at this point is at a higher temperature as a result of the heat transfer already taken place with the preceding surface.

4.1.2. Pressure Profile Results

The pressure values at the inlet and outlet of the heat sink are used to calculate the pressure drop across the heat. The pressure drop value is significant in determining the suitable fan size when designing or purchasing an active heat sink. Since production and retail cost is an influential factor in most engineering designs and inventions, a lower pressure drop is desired, the reasoning behind this is explained in the discussion section below.

$$\Delta P = P_{in} - P_{out} \quad \text{.....Equation (15)}$$

4.2. Simulated Plate Heat Sinks Results

4.2.1. Rectangular Plate Heatsink Results and CAD Model.

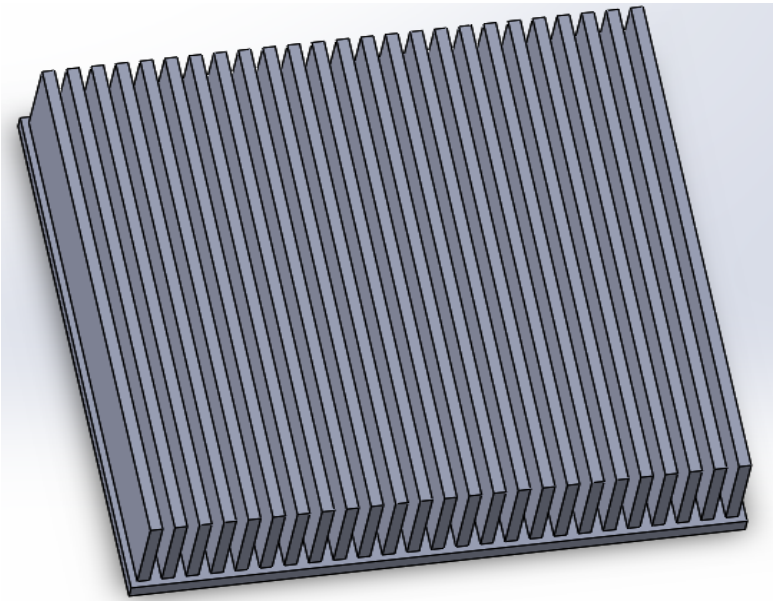

Figure 14: Traditional rectangular heatsink CAD model.

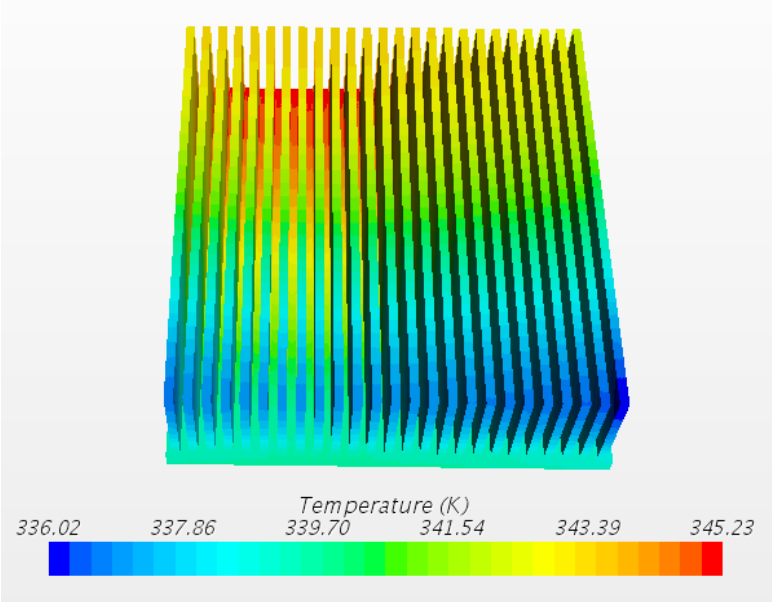

Figure 15: Traditional rectangular plate heatsink temperature result.

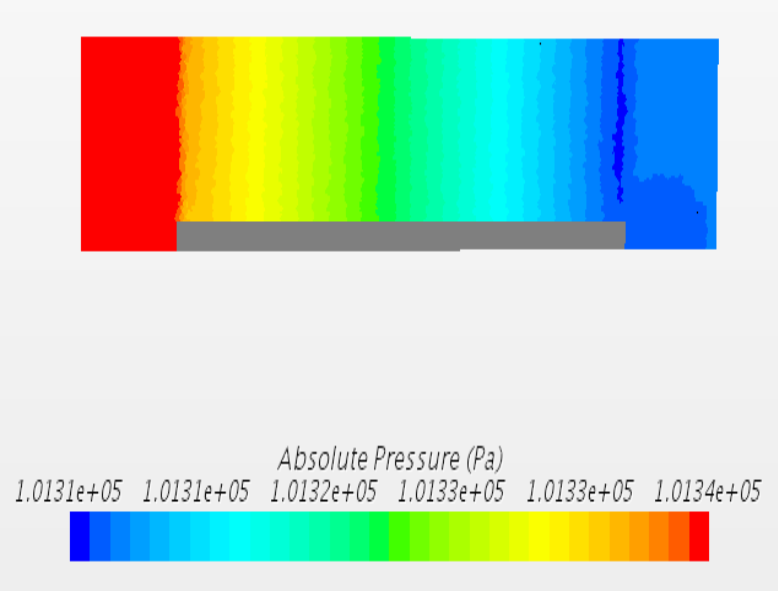

Figure 16: Traditional rectangular plate heatsink pressure result.

4.2.2. Arc Plate Heatsink CAD Model and Result.

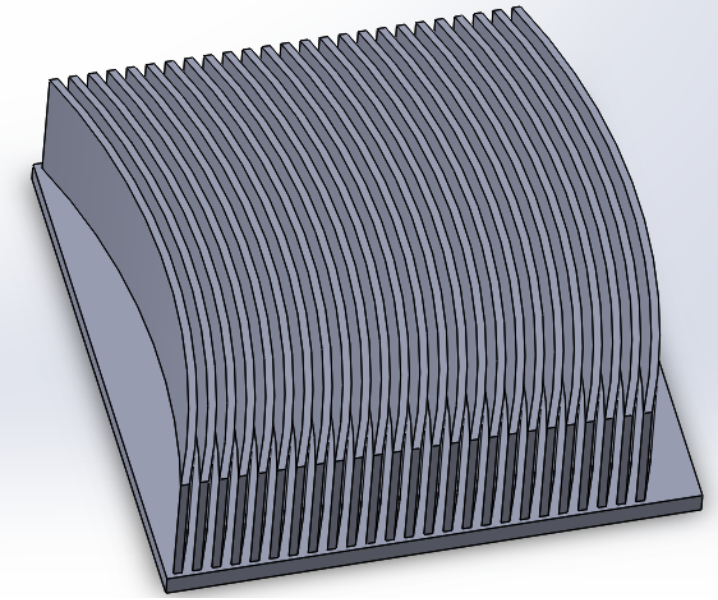

Figure 17: Arc plate heatsink CAD model.

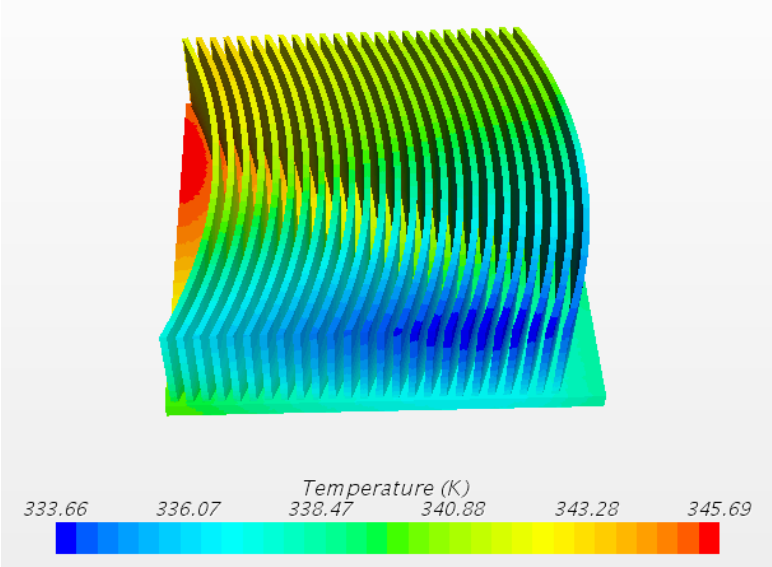

Figure 18: Arc plate heatsink temperature result.

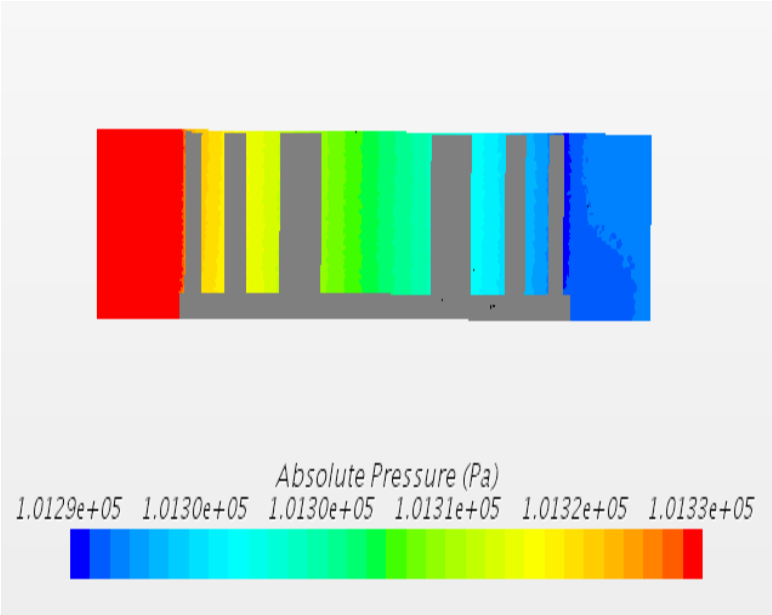

Figure 19: Arc plate heatsink pressure result.

4.2.3. Radial Plate Heatsink CAD Model and Result.

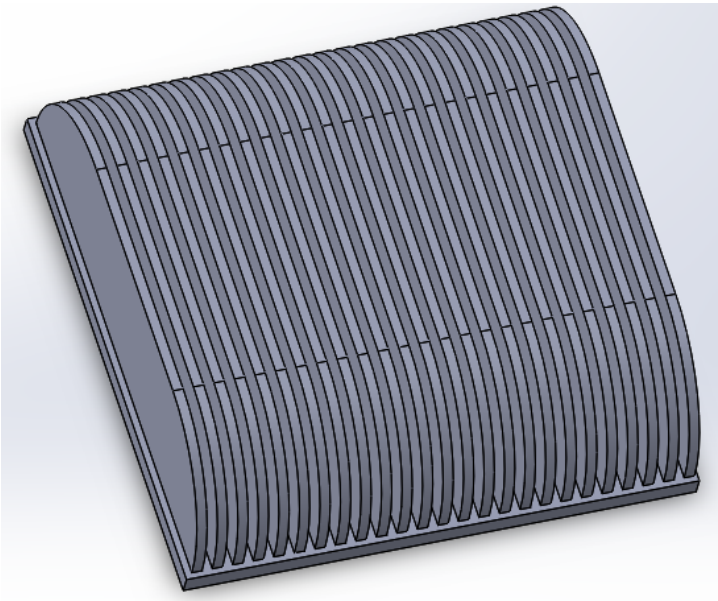

Figure 20: Radial plate heatsink CAD model.

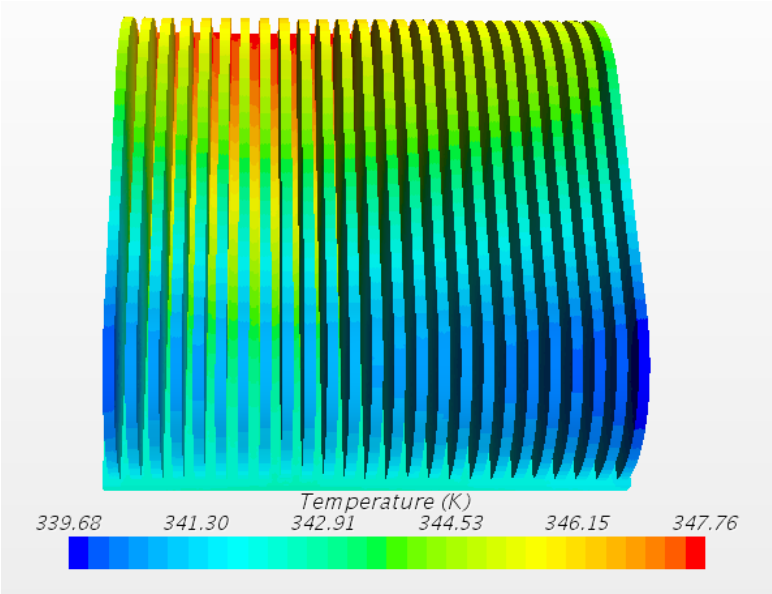

Figure 21: Radial plate heatsink temperature result.

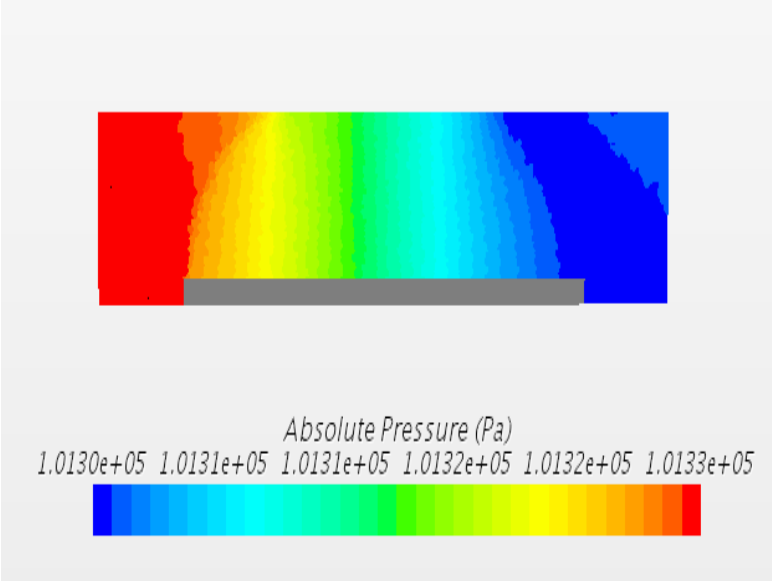

Figure 22: Radial plate heatsink pressure result.

4.2.4. Separated Short Plates Heatsink CAD Model and Result.

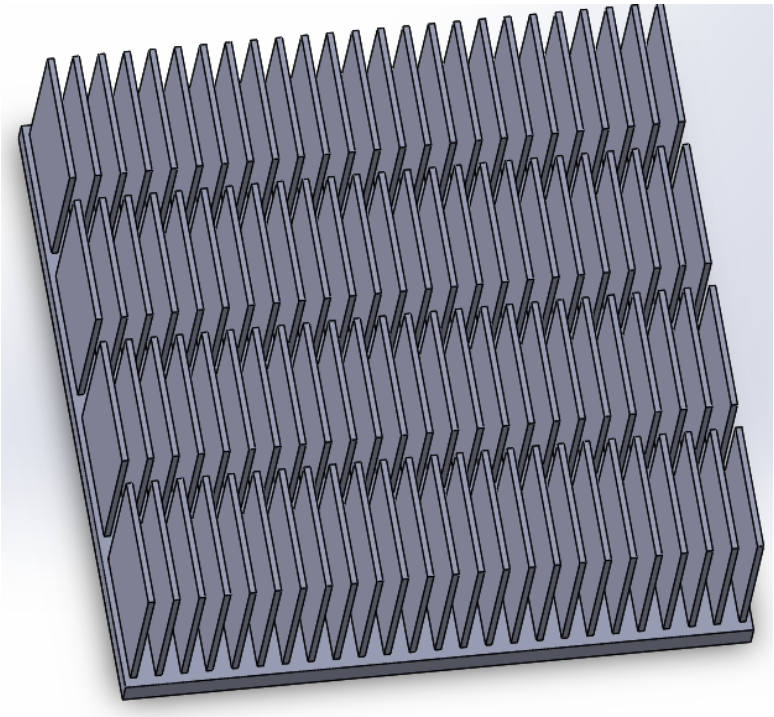

Figure 23: Separated short plates heatsink CAD model.

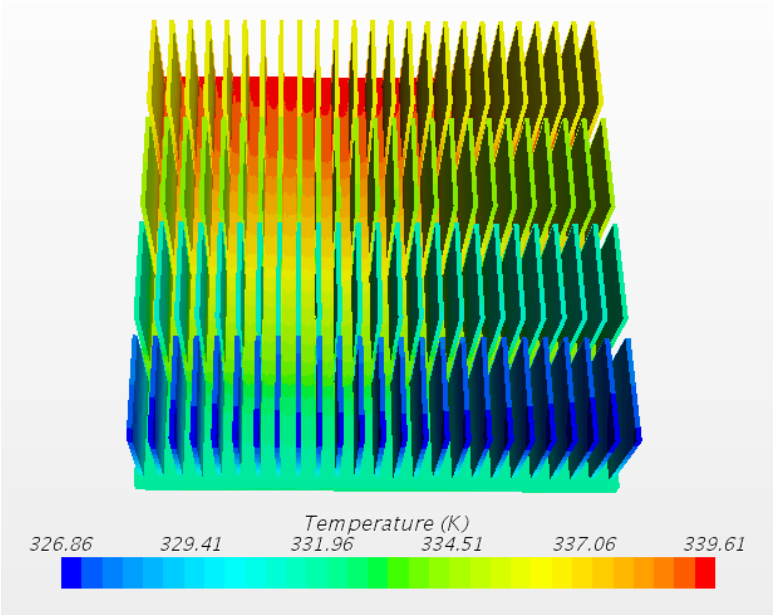

Figure 24: Separated short plates heatsink temperature result.

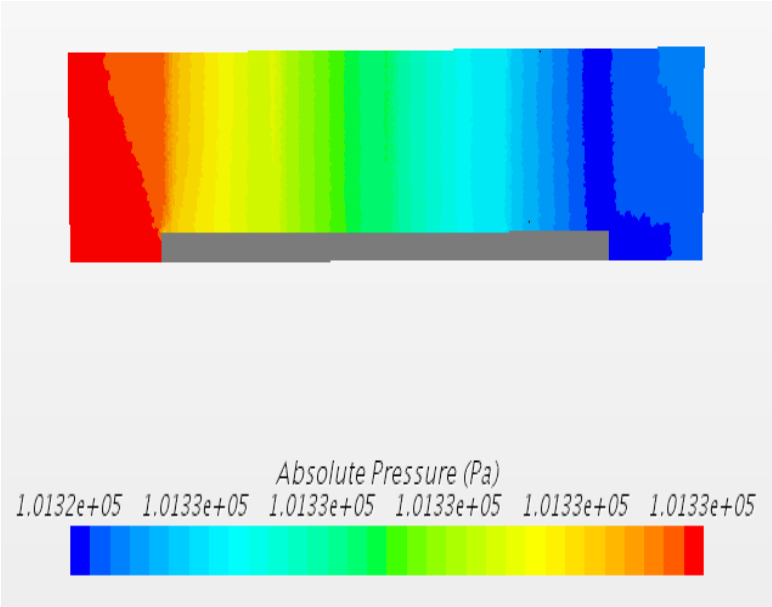

Figure 25: Separated short plates heatsink pressure result.

4.2.5. Airfoil Plate Heatsink CAD Model and Result.

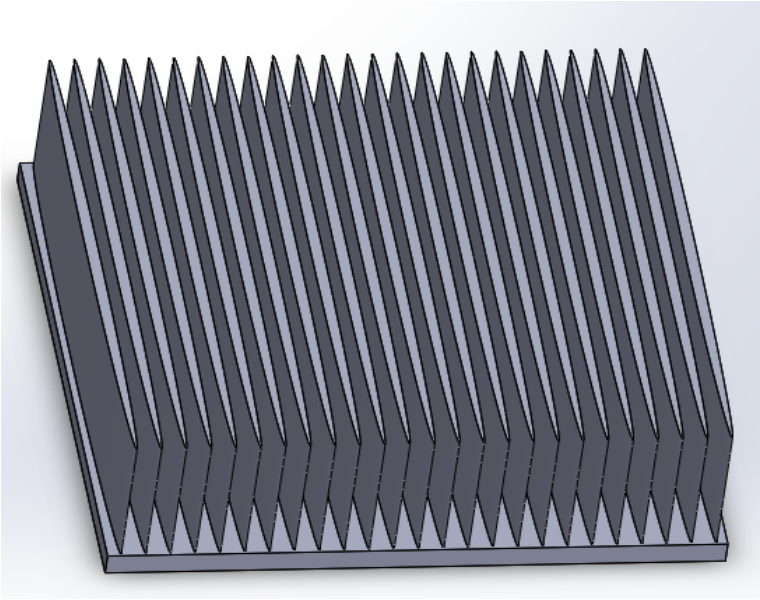

Figure 26: Airfoil plate heatsink CAD model.

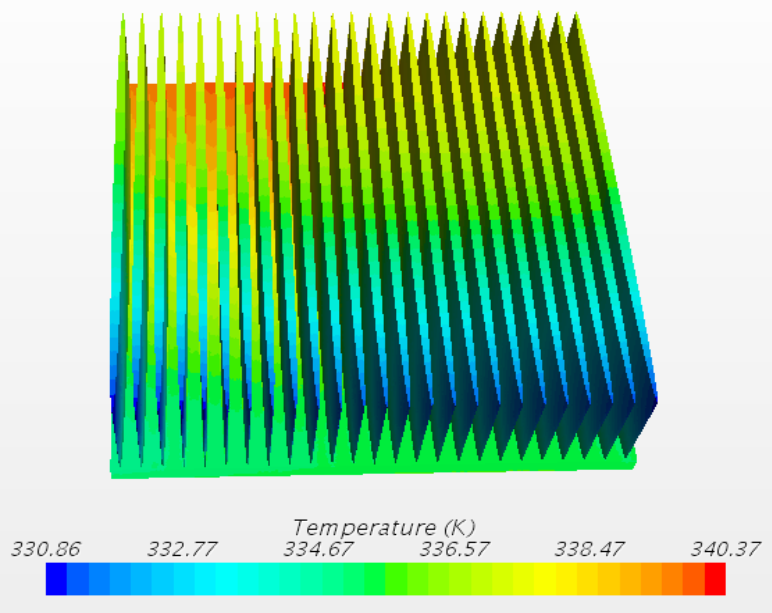

Figure 27: Airfoil plate heatsink temperature result.

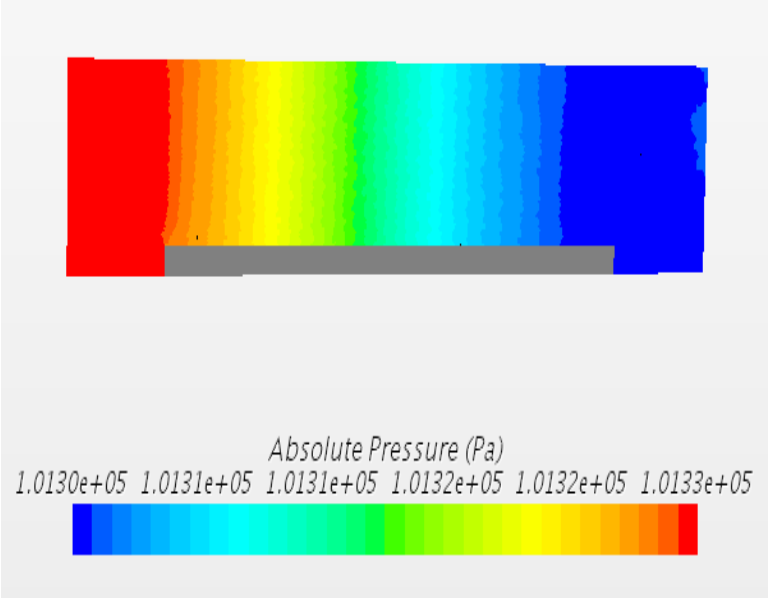

Figure 28: Airfoil plate heatsink pressure result.

4.2.6. Square Zig-Zag Plate Heatsink CAD Model and Result.

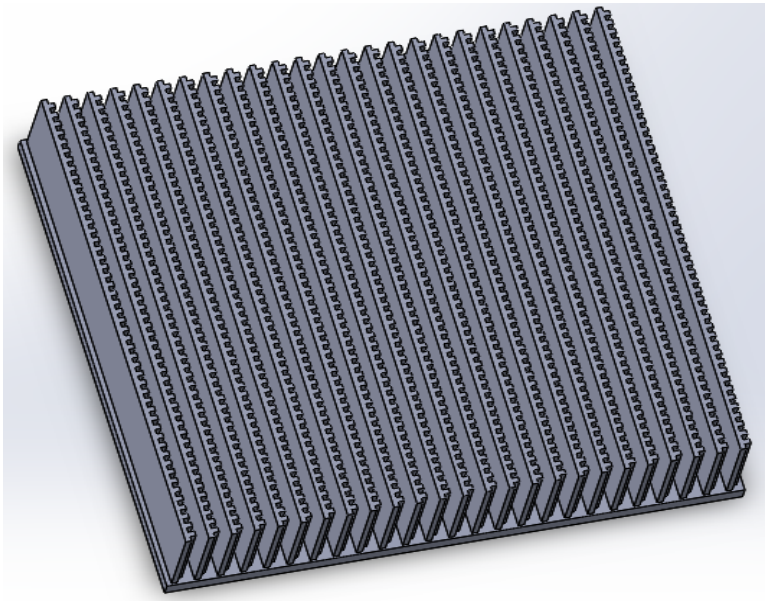

Figure 29: Square Zig-Zag plate heatsink CAD model.

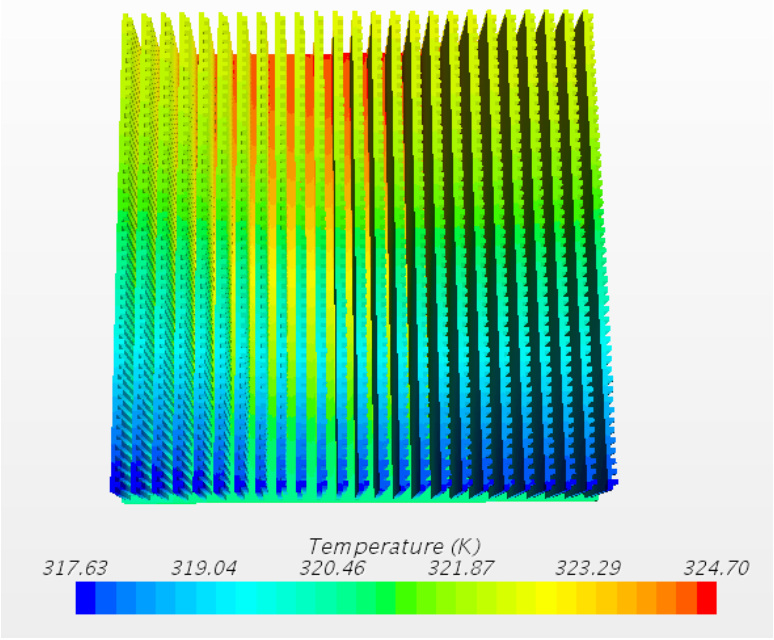

Figure 30: Square Zig-Zag plate heatsink temperature result.

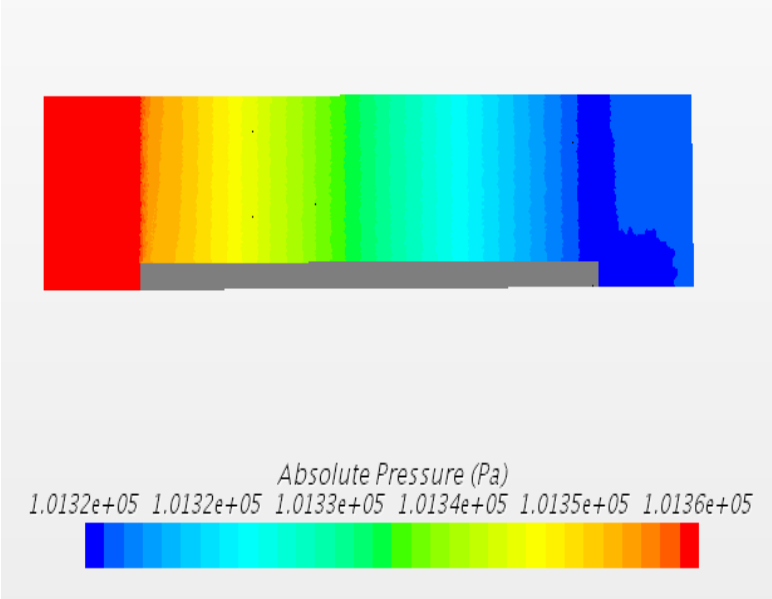

Figure 31: Square Zig-Zag plate heatsink pressure result.

4.2.7. Pin-Plate Heatsink CAD Model and Result.

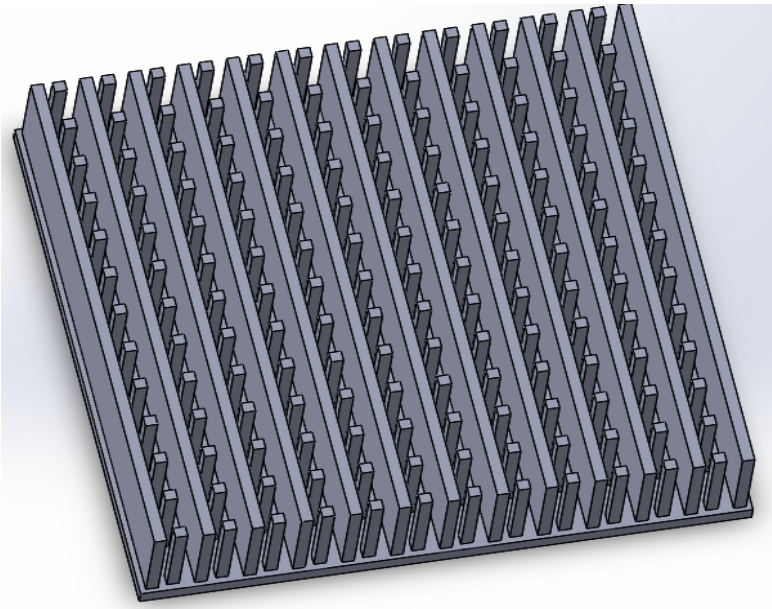

Figure 32: Pin-Plate heatsink CAD model.

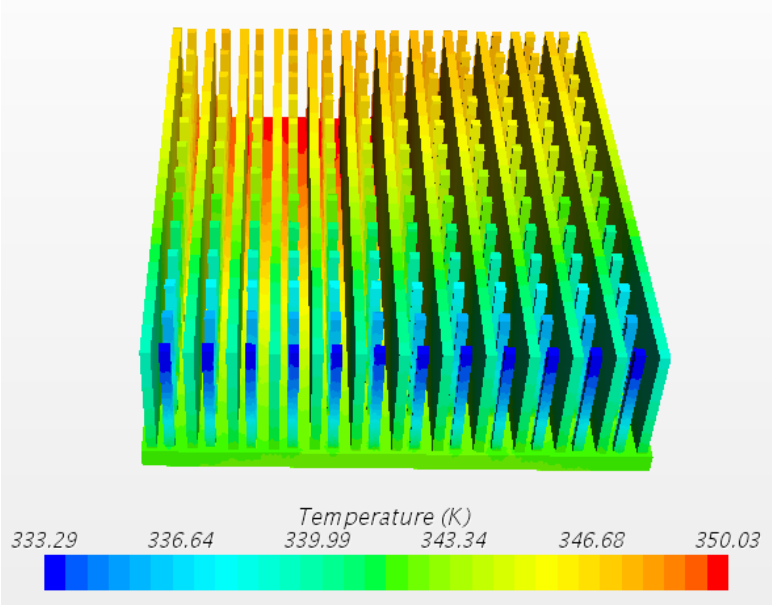

Figure 33: Pin-Plate heatsink temperature result.

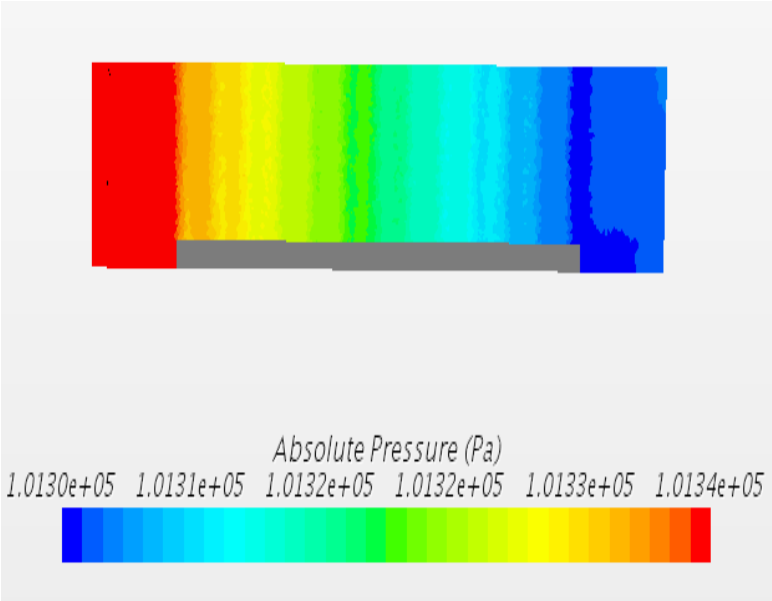

Figure 34: Pin-Plate heatsink pressure result.

4.3. Simulated Pin Heat Sinks Results.

4.3.1. Rectangular Pin heatsink CAD Model and Result.

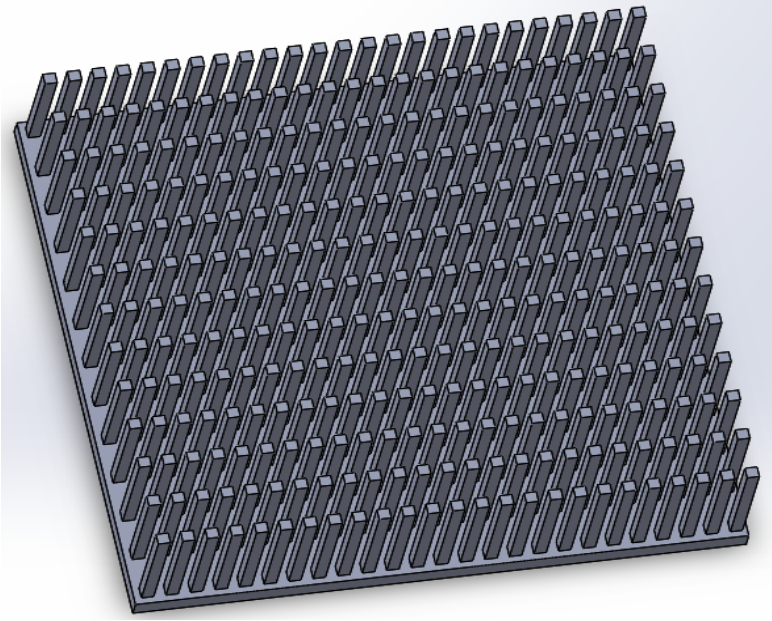

Figure 35: Rectangular pin heatsink CAD model.

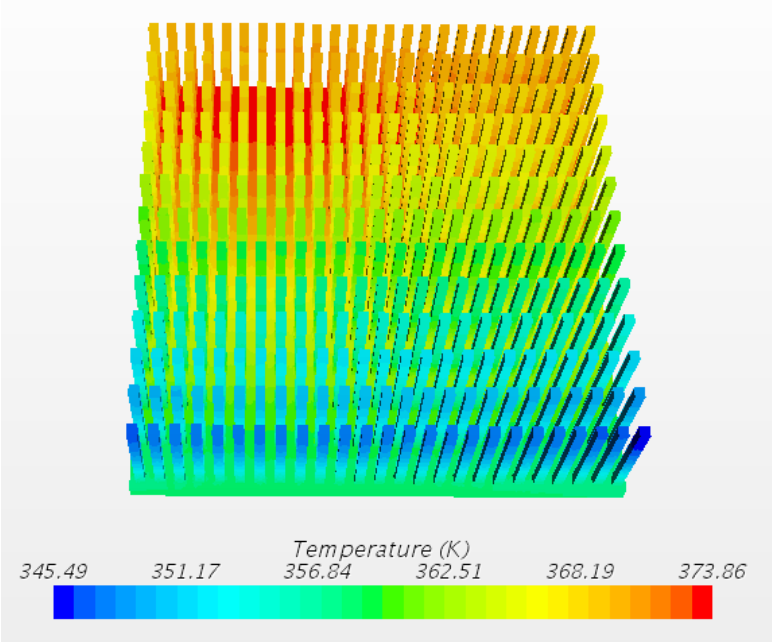

Figure 36: Rectangular pin heatsink temperature result.

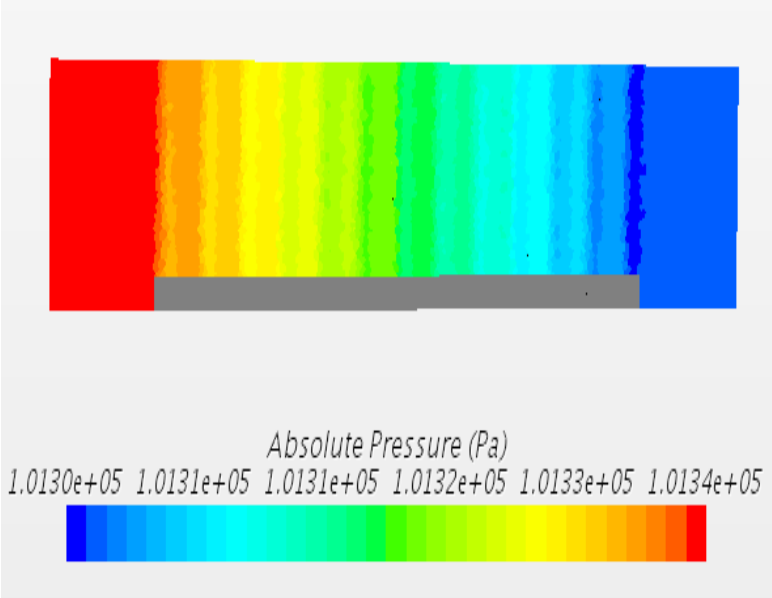

Figure 37: Rectangular pin heatsink pressure result.

4.3.2. Cross Pin heatsink CAD Model and Result.

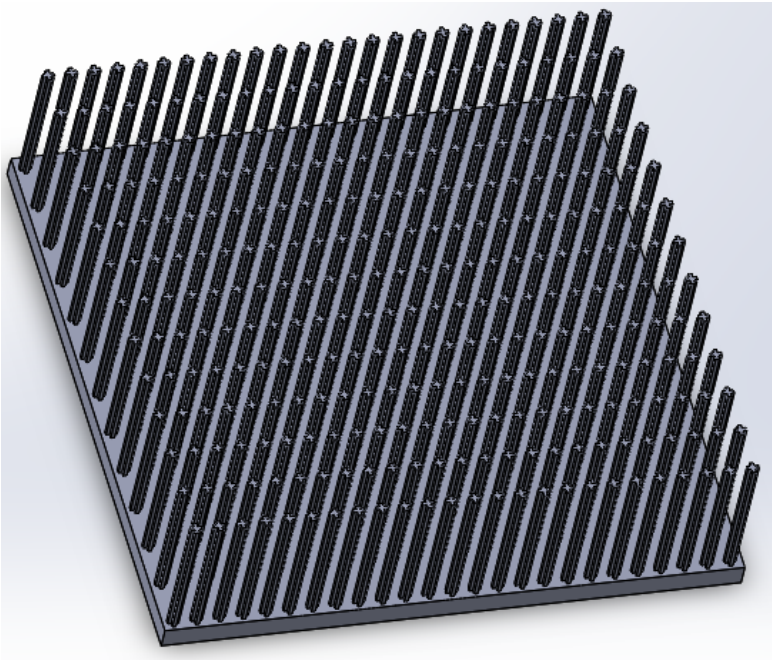

Figure 38: Cross pin heatsink CAD model.

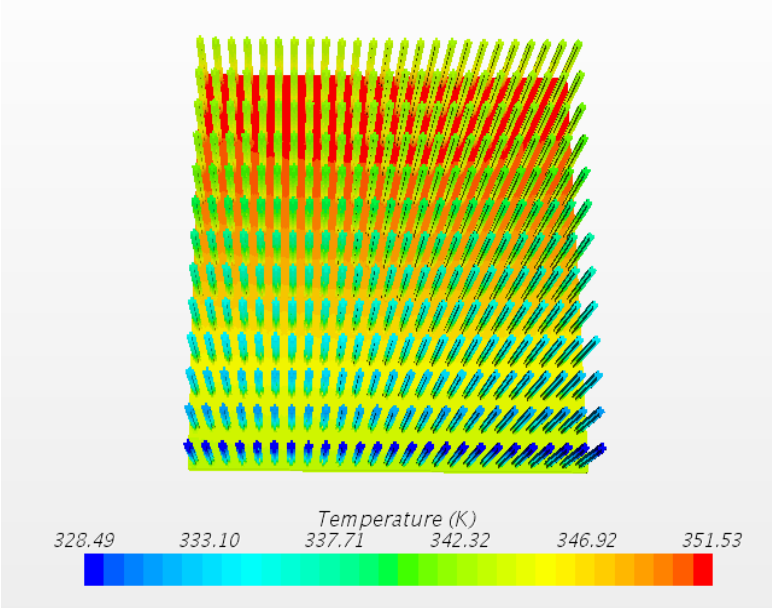

Figure 39: Cross pin heatsink temperature result.

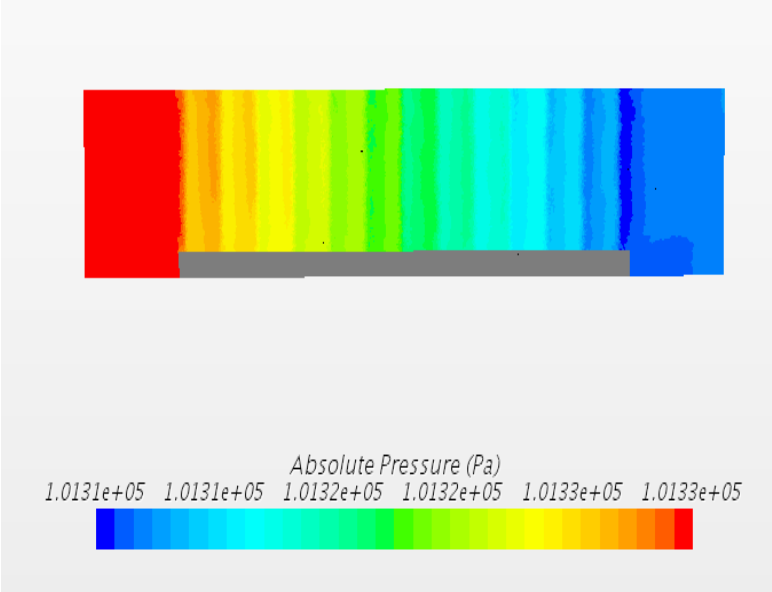

Figure 40: Cross pin heatsink pressure result.

4.3.3. Draft Pin heatsink CAD Model and Result.

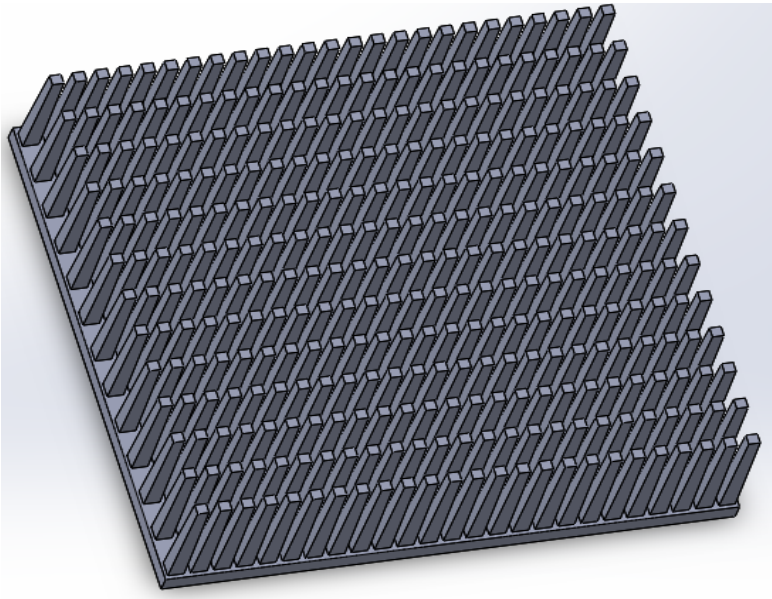

Figure 41: Draft pin heatsink CAD model.

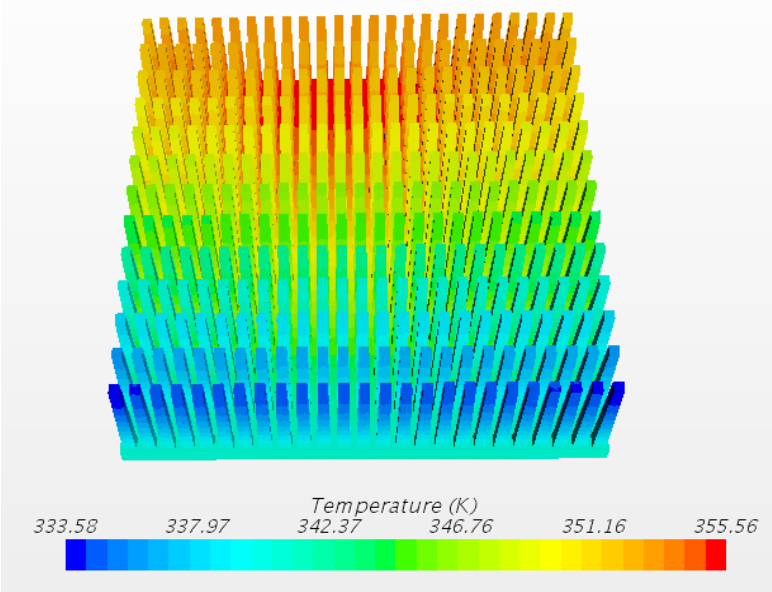

Figure 42: Draft pin heatsink temperature result.

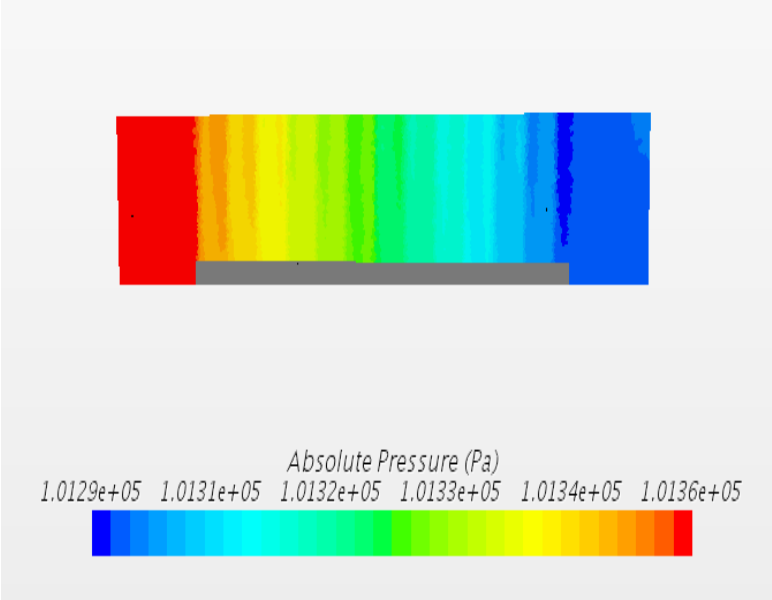

Figure 43: Draft pin heatsink pressure result.

4.3.4. Hexagonal Pin heatsink CAD Model and Result.

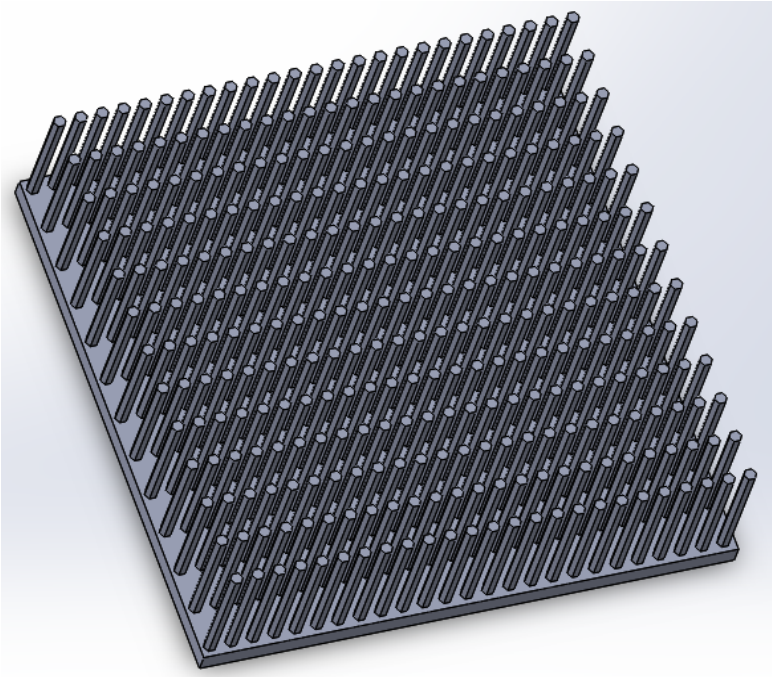

Figure 44: Hexagonal pin heatsink CAD model.

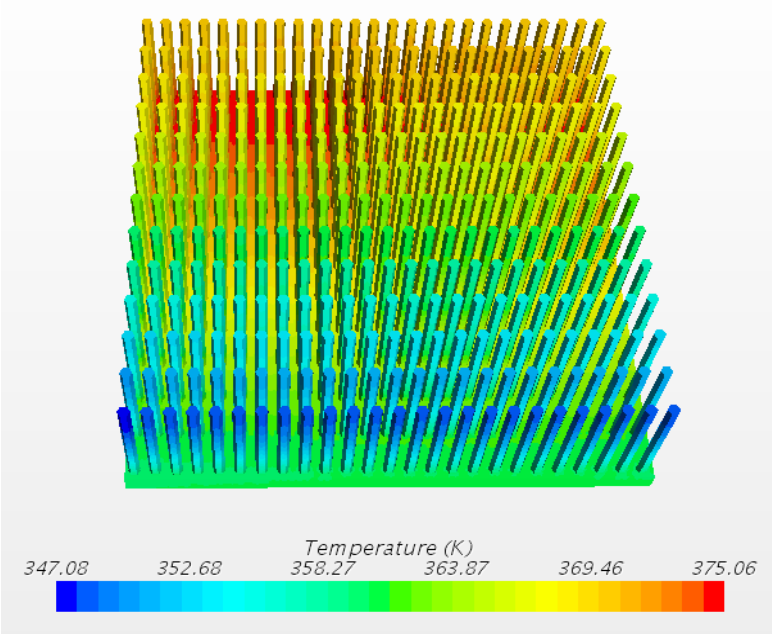

Figure 45: Hexagonal pin heatsink temperature result.

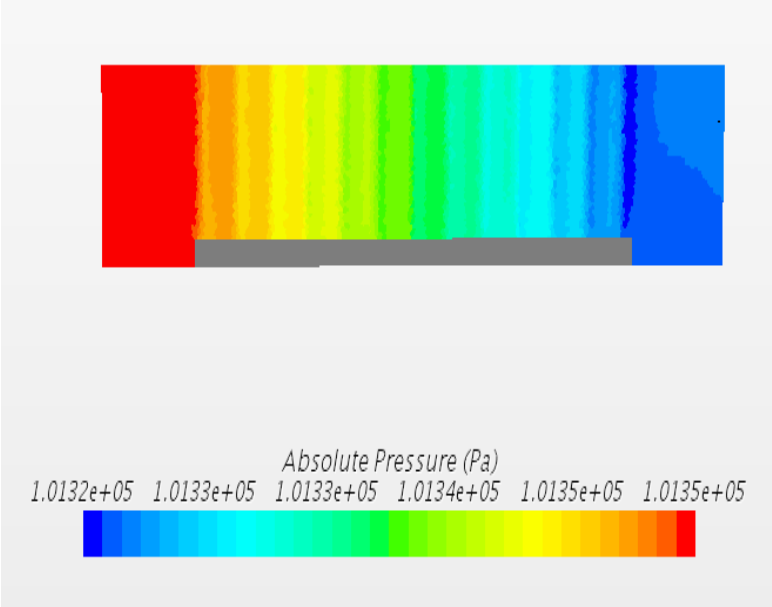

Figure 46: Hexagonal pin heatsink pressure result.

4.3.5. Airfoil Pin heatsink CAD Model and Result.

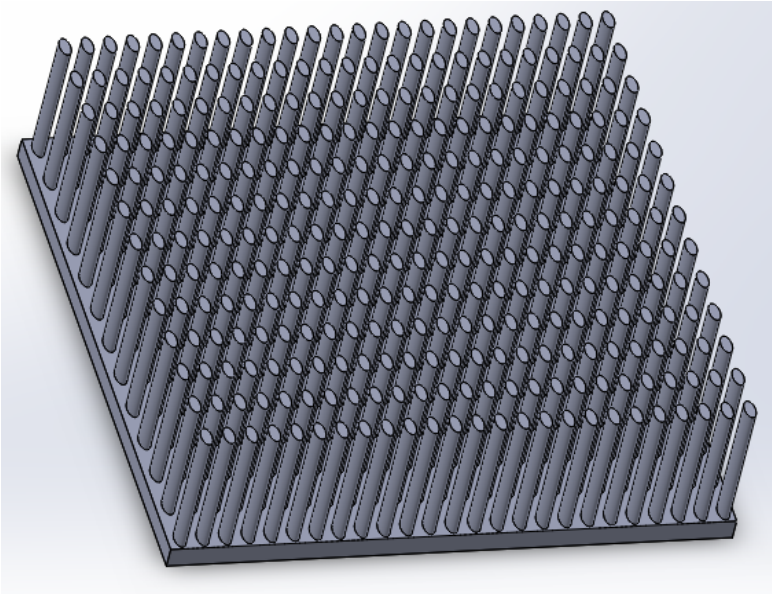

Figure 47: Airfoil pin heatsink CAD model.

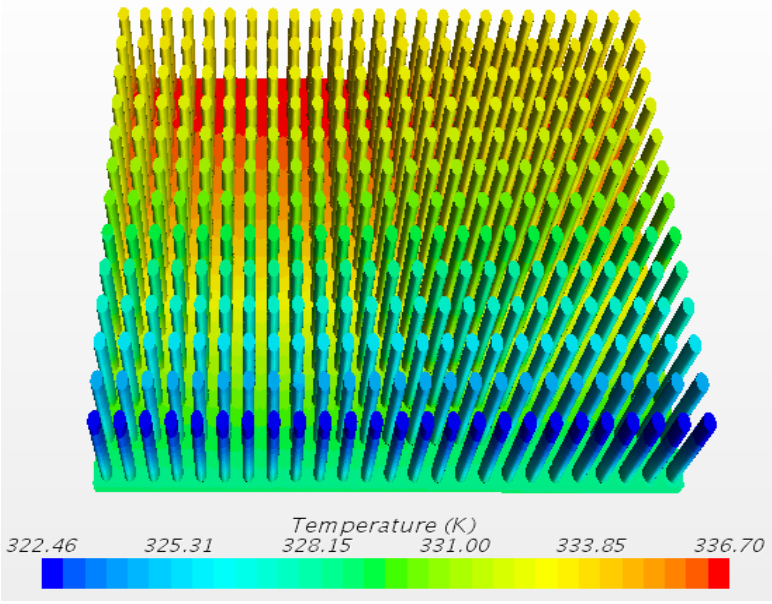

Figure 48: Airfoil pin heatsink temperature result.

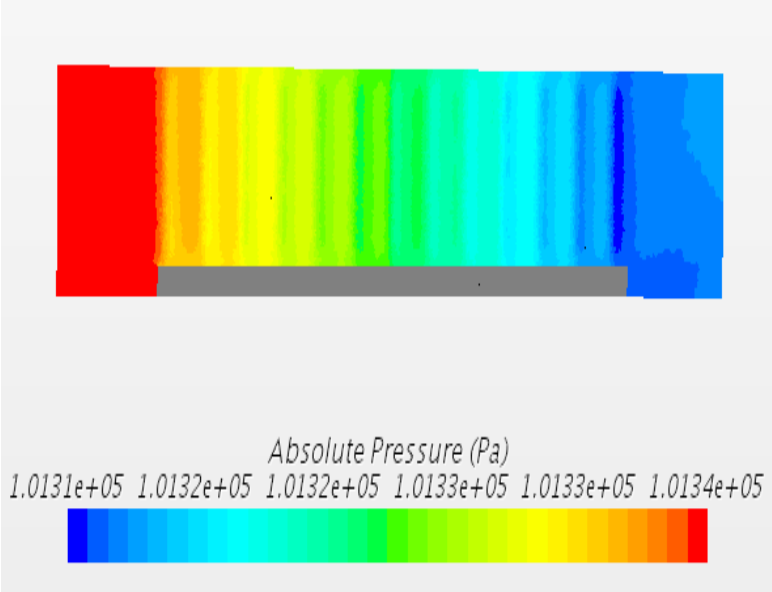

Figure 49: Airfoil pin heatsink pressure result.

4.3.6. Mixed Shapes Pin heatsink CAD Model and Result.

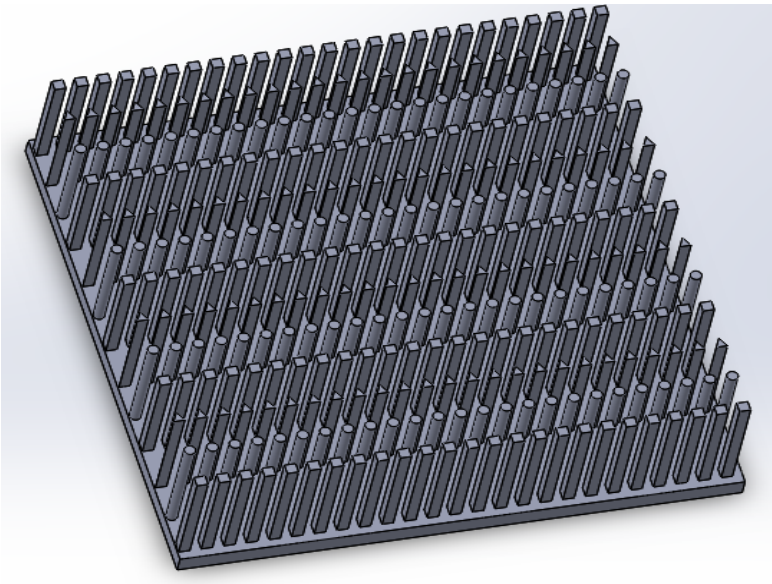

Figure 50: Mixed shapes pin heatsink CAD model.

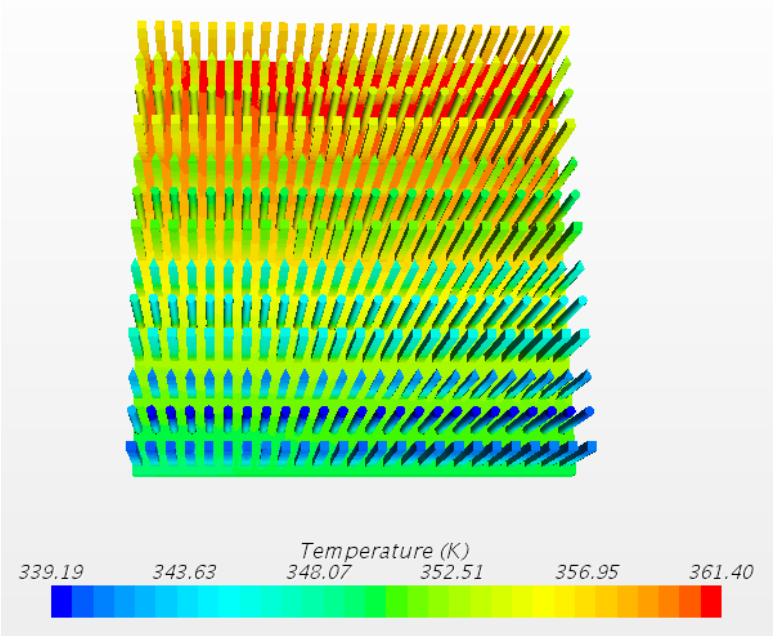

Figure 51: Mixed shapes heatsink temperature result.

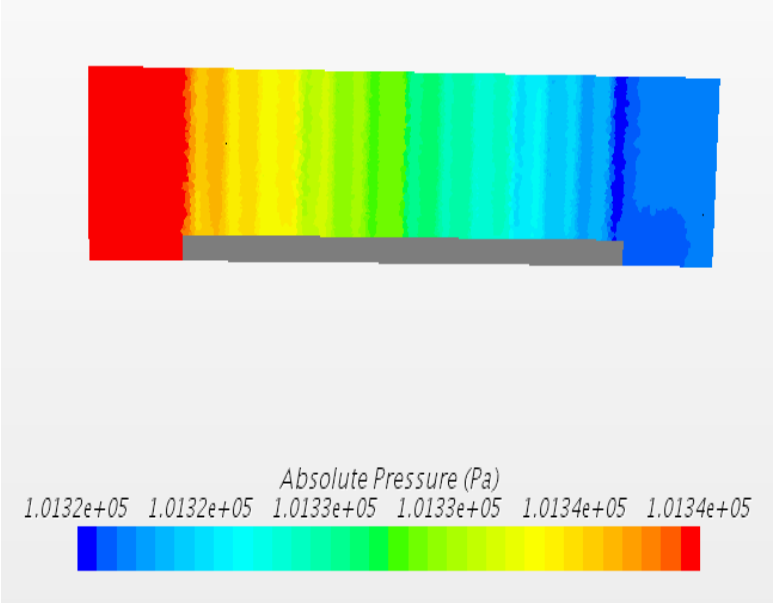

Figure 52: Mixed shapes heatsink pressure result.

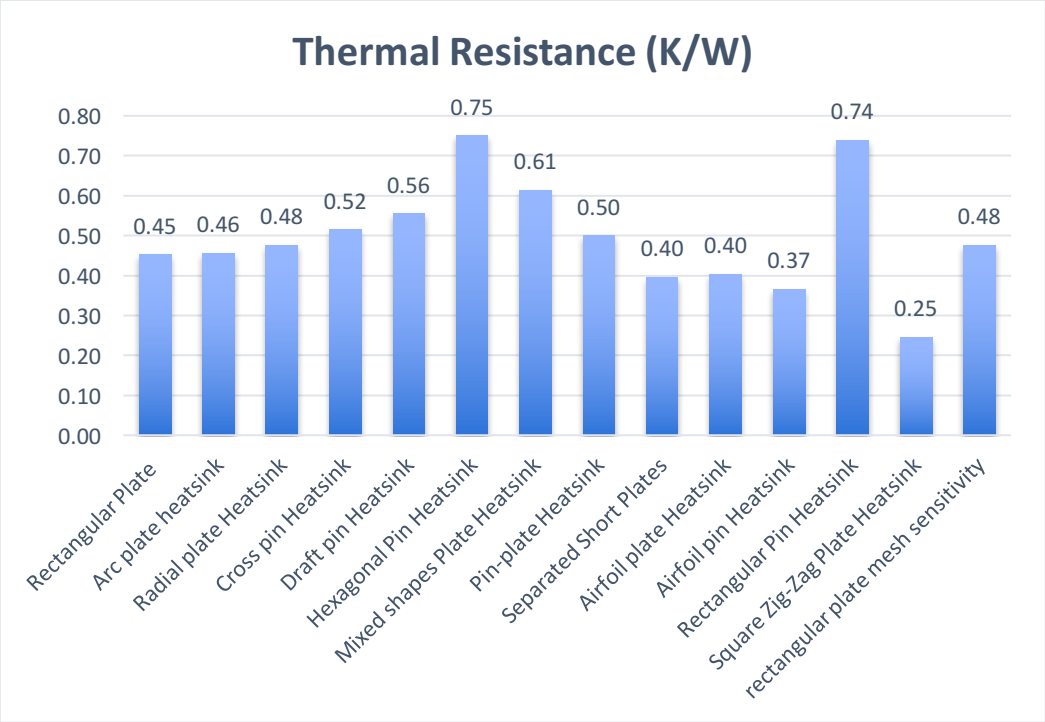

Figure 53: Bar graph showing heatsink and their corresponding thermal resistances.

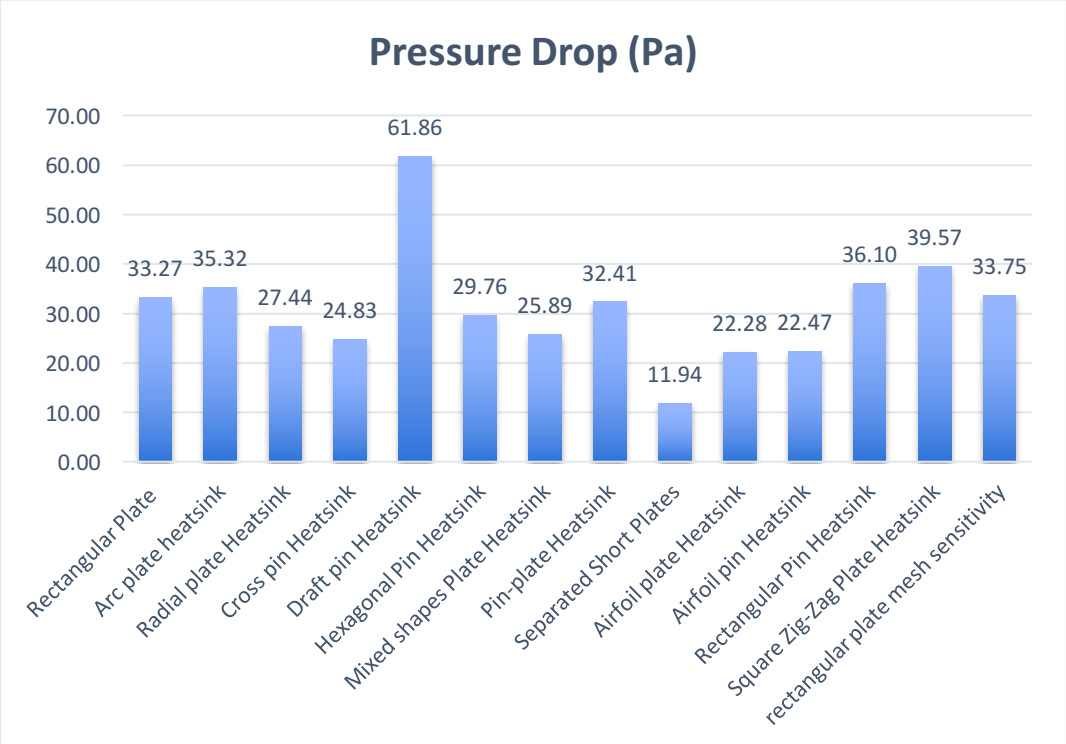

Figure 54: Bar graph showing heatsink and their corresponding pressure drops.

4.4. Result Discussion

Data results from Figure 61 collected from the numerical simulation run was analyzed using bar graphs. For better heatsink performance, a low thermal resistance and pressure drop value is desired. The heatsinks simulated were compared to the traditional rectangular plate heat sink widely used in electronic cooling. Based on the thermal resistance performance parameter of heatsinks, the square zig-zag plate heat sink shown in Figure 29 performed the best. Meaning this heatsink model in comparison to the other heatsinks simulated in this study possessed the least resistance to the transfer of thermal energy between the heatsink (conduction from heat source) to the working fluid(air). The separated short plate heat sink according to the simulation run on the other hand possessed the lowest pressure drop. Meaning, for the heatsink models generated, the separated short plate heatsink requires the smallest (usually cheaper) fan size for operation at the simulation parameters set. This factor is mostly important when the cost of operation in using a heatsink is considered since a bigger fan would usually cost more.

CHAPTER 5: CONCLUSION

The overall goal of this research project was to generate a numerical method of testing different heatsink geometries using CFD software and also generate simple and exotic heatsink fin designs that improve the thermal performance of the heatsink studied in this project. Some proposed models by other researchers in this field were tested for verification. The traditional rectangular plate fin heat sink widely used by thermal engineers for electronic cooling was set as the base of performance comparison since most researchers believe this model heatsink to be efficient both in performance and ease of manufacturability.

The two performance evaluating parameters were thermal resistance and pressure drop. The thermal resistance and pressure drop values for the base case rectangular plate heatsink were 0.45 K/W and 33.27 Pa respectively. Thirteen models were simulated and compared to the rectangular plate fin heatsink. Considering the thermal resistance performance parameter four out of the thirteen models generated performed better. These models and their thermal resistance values are the separated short plates (0.40 K/W), Airfoil plate (0.40 K/W), Airfoil pin (0.37 K/W), and square zig-zag plate (0.25 K/W). For the pressure drop evaluating parameter, eight of the heatsinks tested were found to require a lower pressure drop. These models are the radial plate heatsink (27.44 Pa), cross pin heatsink (24.83 Pa), hexagonal pin heatsink (29.76 Pa), mixed shapes plate heatsink (25.89 Pa), pin-plate heatsink (32.41 Pa), separated short plates heatsink (11.94 Pa), airfoil plate heatsink (22.28 Pa), and airfoil pin heatsink (22.47 Pa).

From the results obtained, it can be concluded that numerical simulation methods/tools including CFD software (STARCCM+) proves to be a cheaper, safer and viable way of testing heatsink performance. Also, with improved manufacturing methods like 3D/ additive printing techniques, complex and exotic heatsink fin models that improve cooling of electronic devices can be manufactured.

CHAPTER 6: FUTURE WORK

Future works include optimizing heat sink performance by running simulations on exotic or more complex heat sink designs using knowledge from heat transfer, fluid mechanics, and additive manufacturing/ 3D manufacturing capabilities. Other suggestions for future work include:

- Conduct study by running simulation using different working fluid.
- Determine the optimal number of fins for both plate and pin fin heat sinks geometries for maximum performance.
- Run CFD simulation with the flow in the Turbulent regime and analyzed the difference in result between laminar regime.
- 3D print and conduct experimental test on heat sink models generated.
- Conduct flow analysis to better understand flow mechanism through the fins of heat sinks.

CHAPTER 7: APPENDIX

7.1. Reynolds-Average Navier-Stokes Equation

The Reynolds-Average Navier Stokes equation represents a method of depicting fluid flow within a system. This equation is derived from the Navier-stokes equation and is capable of predicting the flow velocity without averaging it across a time-step. A combination of the RANS, conservation of mass, and energy equations formulate the basic equations used in modeling practical fluid flows in CFD software tools. With right turbulence models selected this solver or method can be adopted for future work on simulating heatsink models with turbulent flow in STARCCM+.

7.2. Procedure for running heatsink CFD simulation in STARCCM+:

- Generate CAD model in Solidworks or Preferred CAD software.
    - Save file as .x_t or .x_b file. (Parasolid format)
- Import or Load Heatsink file into STARCCM+.
    - Right-click on 3D-CAD Model
        - Import
        - CAD model
- Create Fluid domain around heatsink(solid).
    - Create rectangular sketch around the heatsink.
        - Right-click yz plane
        - Create a sketch to the preferred dimension.
    - Extrude sketch.
        - Right-click on sketch 1
        - Create Extrude

        - Make sure body intersection is “None” for conjugate heat sink method.

- Extract External Volume.
    - Right-Click on Body 2
        - Extract external volume
        - Click OK
- Rename Body parts.
    - Body 1: Solid
    - Delete Body 2
    - Body 3: Fluid
- Name Boundaries.
    - Flow Inlet
    - Flow Outlet
    - Right
    - Left
    - Top
    - Bottom (Fluid region bottom surface)
    - Solid_bottom (Representing heatsink bottom where heat source is applied)
- Load Simulation
    - Close 3D CAD
    - Right click on 3D CAD model
        - New Geometry Part
        - OK
- Assign Parts to Region
    - Right click on Parts under Bodies
    - Fluid
        - Assign Parts to Region

- Make sure to select both fluid and solid
- Click on Create a region for each part and Create boundary for each part surface

- Select Meshing Models
  - Click on Continua
    - Mesh 1
    - Models
    - Select the following meshing Models
      - Surface remesher
      - Polyhedral mesher
      - Generalized cylinder
      - Extruder
      - Embedded thin mesher
    - Click on continua
      - Reference value
        - Base size
          - Select appropriate base size (0.001m)

- Select Physics Models
  - Click on Continua > Select Physics twice for Physics 1(Fluid) and Physics 2 (Solid)
  - Select the following models for Physics 1 (Fluid):
    - Three Dimensional
    - Steady
    - Gas
    - Segregated Flow
    - Gradients
    - Laminar
    - Ideal Gas

        - Segregated Fluid Temperature
        - Gravity
    - Select the following models for Physics 2 (Solid):
        - Constant Density
        - Gradients
        - Segregated Solid Energy
        - Solid
        - Steady
        - Three Dimensional
- Set Physics Continuum for Solid and Fluid region
    - Click on Solid under Regions Tab
        - Change Physics continuum to (Physics 2)
        - Keep Physics continuum of Fluid as (Physics 1)

- Set Boundary Conditions
    - Set Fluid boundary conditions as:
        - Bottom (Wall)
        - Default (Wall)
        - Flow Inlet (Velocity inlet)
        - Left (Symmetry plane)
        - Outlet (Flow-Split Outlet)
        - Right (Symmetry Plane)
        - Top (Symmetry Plane)
    - Set Solid boundary conditions as:
        - Solid_bottom (Thermal Specification > Heat source)
        - Heat Source (100W)
- Run Mesh
    - Click on Cube next to green flag to generate mesh

- Setup Results Display (Scalar Scene)
    - Click on Derived parts>New Part>Section>Plane
- Initialize Solution
    - Click on initialized solution
    - Click run

7.3. Additional validation case heat sink results.

Experimental				
	Velocity (V)	ΔP Pressure Drop(Pa)		
	1	11		
	1.5	18		
	2	25		
	2.5	35		
	3	48		
	3.5	57		
	4	70		
Simulated				
	Velocity (V)	ΔP Pressure Drop(Pa)	Inlet Pressure(Pa)	Outlet Pressure(Pa)
	1	10	101330	101320
	1.5	20	101340	101320
	2	22.5	101342.1	101319.6
	2.5	30.7	101348.3	101317.6
	3	50	101360	101310
	3.5	60	101370	101310
	4	71.9	101380	101308.1

Figure 55: Validation case heatsink numerical and experimental data results.

7.4. Preliminary Results for simple geometry heatsinks simulations run.

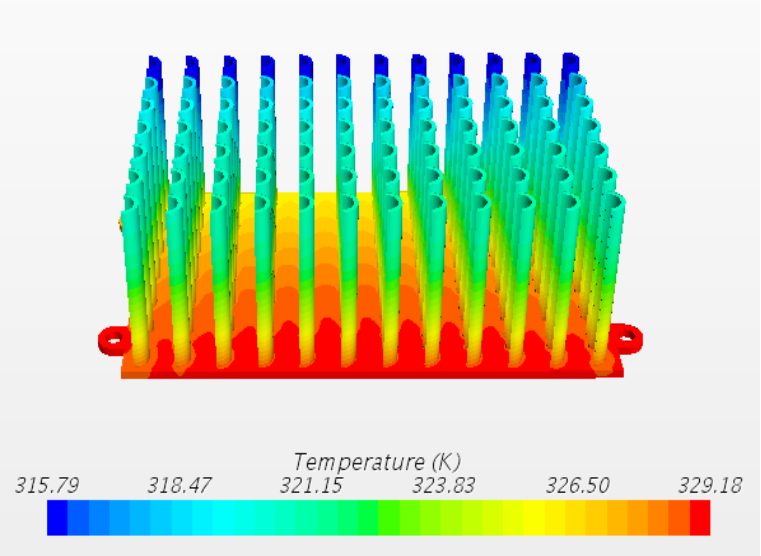

Figure 56: Semi-Circle pin heatsink temperature result.

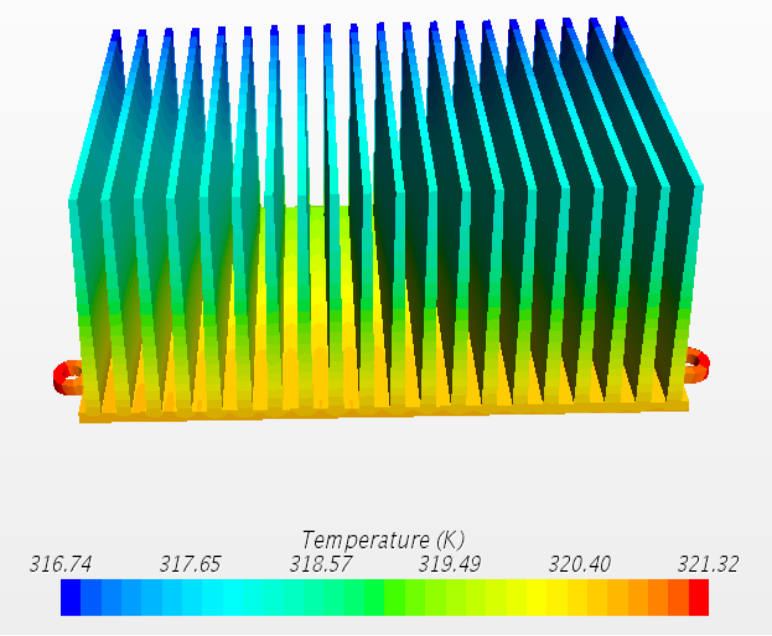

Figure 57: Trapezoidal plate heatsink temperature result.

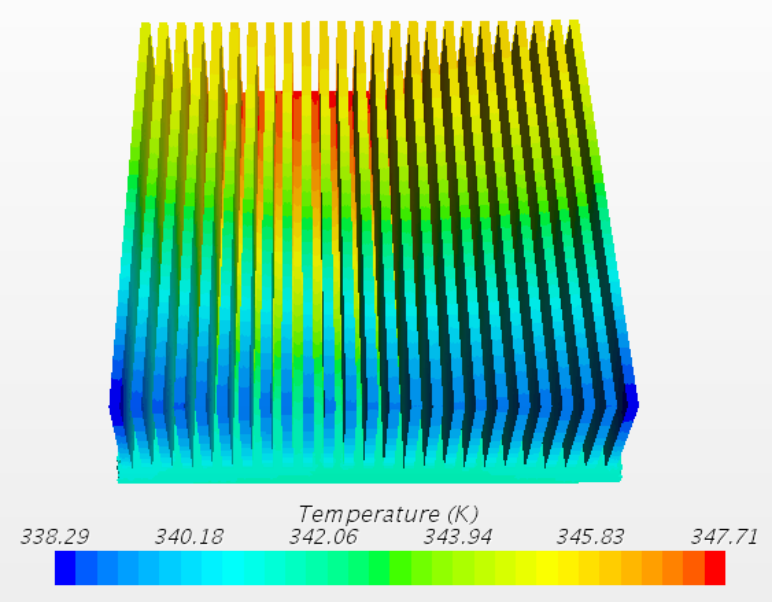

Figure 58: Mesh sensitivity test rectangular plate heatsink temperature result.

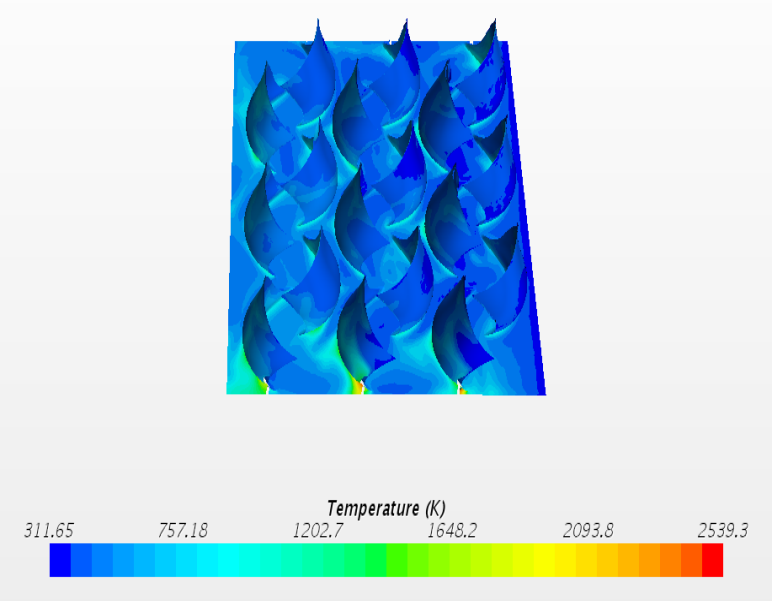

Figure 59: Sample Shark-fin heatsink test simulation results.

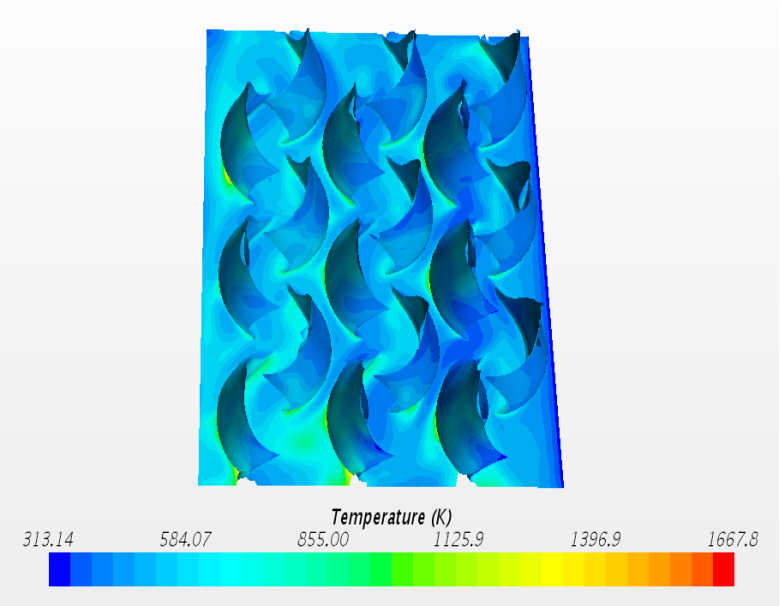

Figure 60: Sample Shark-fin heatsink Test2 simulation temperature result.

Heat sink geometry	Velocity(m/s)	ΔP Pressure Drop(Pa)	Thermal Resistance(K/W)	Inlet Pressure (Pa)	Outlet Pressure(Pa)	Temp 1(K)	Temp 2 (K)	Power(W)	Low temp
Rectangular Plate	1	33.27	0.45	101338.48	101305.21	300	345.228	100	336.018158
Arc plate heatsink	1	35.32	0.46	101325.76	101290.44	300	345.687	100	333.664581
Radial plate Heatsink	1	27.44	0.48	101329.15	101301.72	300	347.764	100	339.680756
Cross pin Heatsink	1	24.83	0.52	101331.65	101306.81	300	351.532	100	328.491547
Draft pin Heatsink	1	61.86	0.56	101356.72	101294.86	300	355.556	100	333.57785
Hexagonal Pin Heatsink	1	29.76	0.75	101351.27	101321.51	300	375.059	100	347.081635
Mixed shapes Plate Heatsink	1	25.89	0.61	101344.95	101319.06	300	361.397	100	339.18512
Pin-plate Heatsink	1	32.41	0.50	101335.34	101302.93	300	350.031	100	333.291443
Separated Short Plates	1	11.94	0.40	101334.95	101323.01	300	339.608	100	326.860931
Airfoil plate Heatsink	1	22.28	0.40	101325.18	101302.90	300	340.369	100	330.864655
Airfoil pin Heatsink	1	22.47	0.37	101336.69	101314.22	300	336.701	100	322.456635
Rectangular Pin Heatsink	1	36.10	0.74	101336.49	101300.39	300	373.863	100	345.49118
Square Zig-Zag Plate Heatsink	1	39.57	0.25	101356.41	101316.84	300	324.700	100	317.630737
rectangular plate mesh sensitivity	1	33.75	0.48	101346.48	101312.73	300	347.709	100	338.294556

Figure 61: Data results from STARCCM+ heatsink simulations.

REFERENCES

[1] S. Lee, M. Early, M. Pellilo, Thermal interface material performance in microelectronics packaging applications, Microelectron. J 28(1) (1997) xiii-xx.

[2] M. A. Ismail, M. Z. Abdullah, and M. A. Mujeebu, 2008, "A CFD-based experimental analysis on the effect of free stream cooling on the performance of micro processor heat sinks," *International Communications in Heat and Mass Transfer,* vol. 35, no. 6, pp. 771-778, 2008.

[3] R. Mohan and P. Govindarajan, 2011, "Experimental and CFD analysis of heat sinks with base plate for CPU cooling," *Journal of Mechanical Science and Technology,* vol. 25, no. 8, pp. 2003-2012,.

[4] ANSYS Fluent Software: CFD Simulation. (n.d.). Retrieved January 18, 2018, from http://www.ansys.com/products/fluids/ansys-fluent.

[5] STAR-CCM. Retrieved January 18, 2018, from https://mdx.plm.automation.siemens.com/star-ccm-plus

[6] S. Subramanyam and K. E. Crowe, 2000, "Rapid design of heat sinks for electronic cooling using computational and experimental tool.," *Institute of Electrical and Electronics Engineers* no. Sixteenth IEEE SEMI-THERM Symposium, p. 8,.

[7] D. Gupta, V. Venkataraman, and R. Nimje, 2014, "CFD & Thermal Analysis of Heat Sink and its Application in CPU.," *International Journal of Emerging Technology and Advanced Engineering* Journal vol. 4, no. 8, p. 5.

[8] X. Yu, J. Feng, Q. Feng, and Q. Wang, 2005, "Development of a plate-pin fin heat sink and its performance comparisons with a plate fin heat sink," *Applied Thermal Engineering,* vol. 25, no. 2-3, pp. 173-182.

[9] 2017, "Advanced thermal solution,". Retrieved January 23, 2018, from, https://www.qats.com/cms/2017/08/22/what-are-benefits-of-using-pin-fin-heat-sinks-in-thermal-management-of-electronics/

[10] Heat Pipe Technology: Passive Heat transfer for Greater Efficiency. Retrieved January 23, 2018, form, http://www.thermacore.com/thermal-basics/heat-pipe-technology.aspx

[11] Korpys M., Dzido G., Wojcik J., 2012, "Experimental and CFD investigation of commercial PC heat sink performance using water and nanofluids.," *14th European Conference on Mixing*, no. 6, pp. 229-234.

[12] Majumder, S., Majumder, A., & Bhaumik, S. (2016). "3-Dimensional numerical study of cooling performance of a heat sink with air-water flow through mini-channel." *American Institute of Physics,* doi: 10.1063/1.49584.

[13] De Stadler, M.B., "Optimization of the Geometry of a Heat sink," University of Virginia, Charlottesville, United States.

[14] Lee, S. Optimum design and selection of heat sinks. *Eleventh IEEE SEMI-THERM Symposium*.

[15] Dogan M., Sivrioglu M., Experimental investigation of mixed convection heat transfer from longitudinal fins in a horizontal rectangular channel: In natural

convection dominated flow regimes, Energy Convers. Manage. 50 (2009) 2513–2521.

[16] Zheng, N., Wirtz, R. A., 1999, “Cylindrical Pin-Fin Fan- sink Heat Transfer and Pressure drop correlations,” *5th ASME/JSME Joint Thermal Engineering Conference*, p.6.

[17] M. Lindstedt, K. Lampio, R. Karvinen, Optimal shapes of straight fins and finned heat sinks, ASME J. Heat Transf. 137(6) (2015) (061006-1-8).

[18] Devansh S., Doom J., 2017, “Simulation of Impinging Jets with a range of configuration,” *American Institute of Aeronautics and Astronautics.*p.12.DOI: 10.2514/6.2017-0751.

[19] Soni A., 2016,” Study of Thermal Performance between Plate-fin, Pin-fin, Elliptical fin Heat sinks in Closed Enclosure under Natural Convection,” *International Advanced Research Journal in Science, Engineering and Technology,* 3(11), pp.133-139. DOI 10.17148/IARJSET.2016.31126.

[20] Lampio, K., & Karvinen, R. (2017). “Optimization of convectively cooled heat sinks,” *Microelectronics Reliability, 79*, 473-479. doi: 10.1016/j.microrel.2017.06.011.

[21] R. Mohan and P. Govindarajan, 2010, "Thermal analysis of CPU with composite pin fin heat sinks," *International Journal of Engineering Science and Technology,* vol. 2(9), pp. 4051-4062,.

[22] Sukumar Sam R., Sriharsha G., Arun Bala S., Dilip kumar P., Ch. Sanyasi Naidu, 2013, "Modelling And Analysis of Heat sink with Rectangular Fins having Through Holes," *International Journal of Engineering Research and Applications (IJERA).*vol 3. Issue (2), pp.1557-1561.

[23] Dede, E. M., Joshi, S. N., & Zhou, F. (2015). Topology Optimization, Additive Layer Manufacturing, and Experimental Testing of an Air-Cooled Heat Sink. *Journal of Mechanical Design, 137*(11). doi:10.1115/1.4030989.

[24] Wits, W. W., Weitkampa, S. J., and van Esb, J., 2013, "Metal Additive Manufacturing of a High-Pressure Micro-Pump," Procedia CIRP, 7, pp. 252–257.

[25] D.B. Tuckerman, R.F.W. Pease, High-performance heat sinking for VLSI, IEEE Electron Device Lett. 2 (5) (1981) 126–129.

[26] Zhang Y., Wang S., Ding P., 2017, "Effects of channel shape on the cooling performance of hybrid micro-channel and slot-jet module", *International Journal of Heat and Mass Transfer*. 113.pp. 295-309.

[27] Barrau J., Chemisana D., Rosell J., L. Tadrist, Ibañez M., 2010, "An experimental study of a new hybrid jet impingement/micro-channel cooling scheme", Appl. Therm. Eng. 30. pp. 2058–2066.

[28] Chen Y., Zhang C., Shi M., Wu J., 2009," Three-dimensional numerical simulation of heat and fluid flow in noncircular microchannel heat sinks", *Int. Commun. Heat Mass Transfer* 36 (9) pp.917–920.

[29] Lee P.S., Garimella S.V., 2006, "Thermally developing flow and heat transfer in rectangular microchannels of different aspect ratios", *Int. J. Heat Mass Transf*. 49 (17–18) pp. 3060–3067.

[30] Lim F.Y., Abdullah S., Ahmad I., 2010, "Numerical Study of Fluid Flow and Heat Transfer in Microchannel Heat Sinks using Anisotropic Porous Media Approximation," *Journal of Applied Sciences*. 10(18): pp. 2047-2057.

[31] Mudawar, 2001, Assessment of high-heat-flux thermal management schemes, IEEE Trans. Compon. Pack. Technol. (2001) 122–141.

[32] Huang, X., Yang, W., Ming, T., Shen, W., & Yu, X., (2017) "Heat transfer enhancement on a microchannel heat sink with impinging jets and dimples".*International Journal of Heat and Mass Transfer, 112*, 113-124. doi:10.1016/j.i.2017.04.078.

[33] Barik A.K., Mukherjee A., Patro P., 2015., "Heat transfer enhancement from a small rectangular channel with different surface protrusions by a turbulent cross flow jet", *Int. J. Therm.* Sci. 98. pp. 32–41.

[34] Feng, S., Shi, M., Yan, H., Sun, S., Li, F., & Lu, T. J. (2018). "Natural convection in a cross-fin heat-sink". *Applied Thermal Engineering. 132*,3037.doi:10.1016/j.applthermaleng.2017.12.049.

[35] Ledezma G., Bejan A., Heat sinks with sloped plate fins in natural and forced convection, Int. J. Heat Mass Transf. 39 (9) (1996). pp.1773–1783.

[36] Kim Dong-Kwon, Thermal optimization of plate-fin heat sinks with fins of variable thickness under natural convection, Int. J. Heat Mass Transf. 55 (4) (2012). pp.752–761.

[37] Elshafei E.A.M.,2010 Natural convection heat transfer from a heat sink with hollow/ perforated circular pin fins, Energy 35 (7) (2010). pp.2870–2877.

[38] Karimpourian B., Mahmoudi J.,2005 "Some Important Considerations in Heatsink Design," *6th International Conference on Thermal, Mechanical and Multiphysics Simulation and Experiments in micro-Electronics and Micro-Systems*, IEEE, pp.406-413.

[39] Iyalla I., Umah K., Hossain M., 2010, "Computational Fluid Modelling of Pipe-Soil Interaction in Current," *World Congress of Engineering.,* 2, p.5. ISSN: 2078-0966.

[40] Solidworks, Retrieved January 23, 2018, from http://www.solidworks.com/

[41] The Midlands Dahlia Society. Retrieved January 23, 2018, from http://www.dahlia-mds.co.uk/Topics/Propagation_2011_6.htm

[42] D. J. C. C.K. Loh, "Comparative Analysis of Heat Sink Pressure Drop Using Different Methodologies.pdf.".p. 6, 2012.

[43] FloTHERM. Retrieved January 23, 2018, from https://www.mentor.com/products/mechanical/flotherm/flotherm/

[44] Thermal Resistance Calculator for Plate Fin Heat Sink. Retrieved January

23, 2018, from https://www.myheatsinks.com/calculate/thermal-resistance-plate-fin/

GLOSSARY

This section of the thesis provides definitions and descriptions of the primary engineering related terms used.

- **Additive Manufacturing/3-D Printing:** process used to create a three-dimensional object by using layers of materials under computational control.
- **Aspect Ratio:** the ratio of width to height.
- **Computational Fluid Dynamics (CFD)**: is a branch of fluid mechanics that uses numerical analysis and data structures to solve and analyze problems that involve fluid flows.
- **Computer Processing Unit**: an electronic component within a computer that carries out instructions that is input into it.
- **Conjugate Heat transfer:** Method of heat transfer modeling that allows simulating of both solid and fluid interaction simultaneously to provide accurate results.
- **Heat Flux:** Amount of heat transfer per unit area to or from a surface.
- **Heat Source:** Object that can heat up another object or space.
- **Kinetic Energy:** energy possessed by an object or body due to its motion.
- **Laminar Flow:** occurs when fluid flows in parallel layers with no disruption between the layers.
- **Mean Absolute Percent error:** Measure of comparing accuracy of results in a study.

- **Nanofluid:** a fluid containing nanometer-sized particles typically made of metals, carbides, oxides, or carbon nanotubes.
- **Nusselt Number:** the ratio of convective to conductive heat transfer across a boundary.
- **Pressure Drop:** difference in pressure between two points within a fluid carrying medium or object. (inlet and outlet).
- **Reynolds Number:** dimensionless quantity used to predict flow patterns in different fluid flow situations.
- **Simulation:** imitation of a situation or process.
- **Thermal Resistance:** the ability of a material or device to resist the flow of thermal energy (heat).
- **Topology:** Study of geometric and space properties that are preserved under continuous deformation.

NOMENCLATURE

A = heat transfer surface area

b = Width of the heat sink gap (m)

CAD = Computer Aided Design

CFD = Computational fluid dynamics

CHT = Conjugate Heat Transfer

CPU = Central Processing Unit

D = Diameter

D_h = Hydraulic diameter (m)

H = Height of fin (m)

f = Fully developed laminar flow friction factor

f_{app} = Apparent friction

K_c = Coefficient of contraction

K_e = Coefficient of expansion

K_H = Kinetic energy

L = Total length of fin (m)

MAPE = Mean Absolute Percent Error (%)

N = Number of fins

$\ominus$ = Thermal impedance

P_{in} = Inlet Pressure (Pa)

P_{out} = Outlet Pressure (Pa)

ΔP = Pressure Drop (Pa)

ρ = Density (kg/m^3)

Q = Power supply (W)

Re = Reynolds Number

T_{base} = base temperature (K)

T_{amb} = ambient temperature (K)

μ = dynamic velocity

V = Velocity (m/s)

V_{ch} = Heat sink channel velocity (m/s)

∇ = Gradient operator